

E. WOLF, PROGRESS IN OPTICS XXXVI
© 1996 ELSEVIER SCIENCE B.V.
ALL RIGHTS RESERVED

II

QUANTUM PHENOMENA IN OPTICAL INTERFEROMETRY

BY

P. HARIHARAN

CSIRO Division of Applied Physics, PO Box 218, Lindfield, New South Wales 2070, Australia

AND

B.C. SANDERS

*School of Mathematics, Physics, Computing and Electronics
and Centre for Lasers and Applications, Macquarie University,
North Ryde, New South Wales 2109, Australia*

CONTENTS

	PAGE
§ 1. INTRODUCTION	51
§ 2. OPTICAL SOURCES	54
§ 3. SECOND-ORDER INTERFERENCE	65
§ 4. THE GEOMETRIC PHASE	73
§ 5. FOURTH-ORDER INTERFERENCE.	78
§ 6. TWO-PHOTON INTERFEROMETRY	91
§ 7. COMPLEMENTARITY	108
§ 8. QUANTUM LIMITS TO INTERFEROMETRY	117
§ 9. CONCLUSIONS	122
REFERENCES	123

§ 1. Introduction

From the time of Young's classical experiment, interference has been regarded as a conclusive demonstration of the wave-like nature of light. However, under appropriate conditions, light also behaves as indivisible particles known as photons. The particle-like behavior of light is particularly noticeable at low light levels, when photo detectors register distinct events corresponding to the annihilation of individual photons. At the single-photon level, quantum effects cannot be ignored.

1.1. QUANTUM EFFECTS

What are quantum effects? The answer lies in an understanding of complementarity. Under appropriate conditions, light can be treated as a wave, subject to the behavior dictated by Maxwell's equations; in other situations, light seems to be composed of localized particles. As delocalization is necessary for interference to occur, these two views of light are incompatible. Nevertheless, the two views do apply to light from the same source, and this contention is supported by experimental evidence. This dichotomy is the essence of the quantum nature of light: not that light is a particle or a wave, but rather that light exhibits the characteristics of both a particle and a wave, leading to Dirac's famous statement that "... each photon interferes only with itself. Interference between different photons never occurs" (Dirac [1958]).

1.2. COMPLEMENTARITY

The paradox presented by something that is both corpuscular and undular is avoided by the existence of a complementarity principle in measurements. This principle of complementarity limits the possibility of performing a measurement which *simultaneously* demonstrates both undular and corpuscular behavior. We can, of course, use the same source of light first to observe particles and then to observe waves, and *vice versa*, but we cannot take the same "piece of light" and check one feature without altering, or demolishing, the other.

A way to resolve this paradox has been interference experiments at low light levels, using beams of light with low photon numbers. These experiments can be categorized according to the light source used, the manipulation of the beams and the detection technique. By permuting the various possibilities, experiments can be performed to explore a range of quantum phenomena.

1.3. SECOND-ORDER COHERENCE

The optical field can be characterized completely by the expectation values of various powers and products of the field variables, beginning with the second-order coherence (Wolf [1955]).

Second-order coherence corresponds to measurements of complex amplitudes for the field at two space-time points using interferometers, such as the Michelson and Mach-Zehnder interferometers, which produce interference fringes by mixing two fields with differing phases. The usual way to do this is by varying the optical path difference, but an alternative method is by operating on the geometric phase (Berry [1984, 1987]).

We first review experiments of this type which explore the quantum nature of light, ranging from early experiments involving low-intensity sources and fields from independent sources at low intensity levels, to measurements using nonclassical light sources, including single-photon states and photon-pair sources. The wave-like behavior of light is made clear by accumulating enough single-photon events; the corpuscular aspect is revealed by determining the path of the photon. For the photon to produce interference fringes, it must interfere with itself, a condition which requires the photon to traverse both paths; yet a direct measurement of the photon in either path should, by the principle of complementarity, reveal that the photon has localized itself to one path or the other. “Which path” (*welcher Weg*) measurements verify that the photon is indeed localized to one path or the other when an inspection is carried out, despite the fact that the photon can interfere with itself in the absence of an inspection.

1.4. NONCLASSICAL STATES OF LIGHT

A precise distinction between semiclassical and nonclassical states of light can be made by expanding the quantum field state in the Glauber coherent-state basis (Glauber [1963a,b]). If the corresponding c -number quasiprobability distribution, the Glauber-Sudarshan P -representation (Glauber [1963a,b], Sudarshan [1963]), satisfies the requirements of a probability distribution, namely that it is nonnegative and normalized to unity, then the state is referred to as a

classical state of light. A purely quantum state produces a Glauber–Sudarshan P -representation which does not satisfy the criteria for a probability distribution.

1.5. FOURTH-ORDER COHERENCE

Measurements of second-order coherence cannot unambiguously distinguish a classical state of light from a quantum state. However, fourth-order coherence measurements, which correspond to intensity correlation measurements, permit quantum states of light to be distinguished from classical states. In the simplest conceptual form of these experiments, a single photon is directed at a beam splitter. A measurement at the two output ports of the beam splitter should, under ideal circumstances, detect the photon in either output port, whereas a classical field would be split between the two. The fourth-order coherence function is sensitive to the fact that the photon cannot be split into two regions of space, and there exists a range of values for fourth-order coherence measurements which are attainable for quantum states of light, but not for classical states of light. Besides providing unambiguous evidence for the existence of nonclassical light, fourth-order coherence experiments often present phenomena which appear counterintuitive.

1.6. ENTANGLED STATES

Correlated photon pairs produced by parametric down-conversion make possible a variety of experiments by which to probe the quantum mystery. The two photons are produced in an entangled state leading to a situation where observations on either photon separately reveal no interference, but observations involving coincidences of the two photons yield higher-order interference fringes.

Tests of Bell's inequality (Bell [1965]) play a crucial role in ruling out local realism as an alternative framework for describing quantum effects. Two-photon interferometry using entangled states makes it possible to carry out such tests without invoking polarization. Another series of experiments on two-photon interferometry vindicates Feynman's proposition that states interfere with each other only when they cannot be distinguished physically in the experimental setup. Yet another series of experiments has demonstrated the idea of a "quantum eraser", in which it is possible to appear to destroy "which-path" information without actually doing so.

1.7. BEAM-SPLITTING AND TUNNELING

As mentioned earlier, any description of light involving waves predicts that there will be some coincidences between photon detectors placed in the two output fields produced by a beam splitter. On the other hand, for single-photon states, quantum theory predicts, and experiments confirm, the probability of coincidences to be zero.

In a variant of these experiments, the beam splitter is replaced by two prisms with a very small air gap between them. It is then possible, with single-photon states, to observe particle behavior (anticoincidence) and wave behavior (tunneling) in the same apparatus.

A related question is the time taken by a photon to tunnel through such a barrier. Experiments using two-photon interference have revealed such puzzling effects as apparently superluminal tunneling velocities.

1.8. QUANTUM LIMITS

Finally, quantum effects set a limit to the precision attainable in measurements using interferometry. The complementarity of particle and wave aspects is responsible for an uncertainty principle linking the photon number and the measured phase. However, it does appear possible to perform measurements with precision beyond the standard quantum limit (SQL), either by injecting nonclassical light into the interferometer or by replacing passive optical elements in the interferometer by active nonlinear elements.

§ 2. Optical Sources

The earliest sources of light for interference experiments were thermal light sources, such as the sun and incandescent light. They have been supplemented by the laser, a source of coherent light, and, more recently, by atomic sources and nonlinear optical materials which provide nonclassical light.

Coherence functions have been used for many years to characterize classical light fields (Wolf [1955]), but Glauber [1963a,b] was the first to construct the quantum analog of classical coherence functions to characterize the coherence properties of nonclassical radiation. An important realization was that measurements of second-order coherence¹ cannot provide unambiguous evidence of

¹ Glauber [1963a,b] refers to this function as the first-order correlation.

nonclassical light; measurements of fourth-order coherence, at the very least, are required to distinguish nonclassical from classical radiation.

2.1. QUANTUM DESCRIPTION OF RADIATION

By analogy with the coherence functions used to describe the interference properties of the classical radiation field, Glauber [1963a,b] introduced the normalized quantum coherence functions to describe the quantum field. The electric field at the space-time point (\vec{r}_i, t_i) is replaced by the operator $\hat{E}(\vec{r}_i, t_i)$, which can be separated into negative- and positive-frequency components, $\hat{E}^-(\vec{r}_i, t_i)$ and $\hat{E}^+(\vec{r}_i, t_i)$, respectively. What would be referred to, in classical terms, as the normalized coherence functions of order $2n$ are then defined as the correlation functions of order n :

$$g^{(n)}(\{\vec{r}_i, t_i | i = 1, \dots, 2n\}) = \frac{\langle : \prod_{i=1}^n \hat{E}^-(\vec{r}_i, t_i) \prod_{i=n+1}^{2n} \hat{E}^+(\vec{r}_i, t_i) : \rangle}{\prod_{i=1}^{2n} \sqrt{\langle \hat{E}^-(\vec{r}_i, t_i) \hat{E}^+(\vec{r}_i, t_i) \rangle}}, \quad (2.1)$$

where $: :$ represents the normal-ordering operation, and the angular brackets refer to both ensemble averaging and to quantum state averaging. Whereas $0 \leq g^{(1)}(\{\vec{r}_i, t_i | i = 1, 2\}) \leq 1$ for both quantum and classical radiation fields, the second-order correlation function satisfies the criteria

$$1 \leq g^{(2)}(\{\vec{r}_i, t_i | i = 1, \dots, 4\}) < \infty \quad \text{for a classical field,} \quad (2.2)$$

$$0 \leq g^{(2)}(\{\vec{r}_i, t_i | i = 1, \dots, 4\}) < \infty \quad \text{for a quantum field.} \quad (2.3)$$

Hence, values of second-order correlation in the range

$$0 \leq g^{(2)}(\{\vec{r}_i, t_i | i = 1, \dots, 4\}) < 1 \quad (2.4)$$

indicate unambiguously a nonclassical light source.

In addition to using the quantum correlation functions, it is important to describe the field in terms of quantum states. The field emitted by the source can be decomposed into arbitrary modes indexed by the three-vector \vec{k} , which, for a plane wave, is the wave vector.

We represent the n -photon state in mode \vec{k} by the expression

$$|n\rangle_{\vec{k}} \equiv (n!)^{-1/2} \left(\hat{a}_{\vec{k}}^\dagger \right)^n |0\rangle, \quad (2.5)$$

in which $|0\rangle$ designates the zero-photon state or ground state, of the field mode, corresponding to the vacuum state, and the subscript \vec{k} can be ignored where not required.

The nonclassical nature of the n -photon state is made evident when we calculate the second-order correlation function,

$$g^{(2)}(0) = 1 - \frac{1}{n}, \quad (2.6)$$

which, from eq. (2.4), is within the nonclassical regime. For $n=1$, the interpretation of eq. (2.6) is particularly straightforward: the photon is indivisible, and fractions of the photon cannot be detected at different space-time points.

The bridge between the classical and quantum descriptions of radiation is provided by the coherent state of light,

$$|\alpha\rangle = \exp\left(-\frac{1}{2}|\alpha|^2\right) \sum_{n=0}^{\infty} \frac{\alpha^n}{\sqrt{n!}} |n\rangle, \quad (2.7)$$

which has complex amplitude α and mean photon number $|\alpha|^2$. This coherent state of light is indistinguishable from classical coherent light: all orders of the correlation function defined by eq. (2.1) are equal to unity for the coherent state defined by eq. (2.7).

Classical radiation states can be expressed in the quantum framework as distributions of coherent states of light. Thus, the density matrix for the light field can be written as:

$$\hat{\rho} = \int d^2\alpha P(\alpha) |\alpha\rangle \langle\alpha|, \quad (2.8)$$

where $P(\alpha)$ is referred to as the Glauber–Sudarshan P -representation after the work of Glauber [1963a,b] and Sudarshan [1963], and the classical radiation states are diagonal in the overcomplete coherent-state basis. The P -representation for the coherent state $|\alpha_0\rangle \langle\alpha_0|$ is evidently $P(\alpha) = \delta^{(2)}(\alpha - \alpha_0)$, where $\delta^{(2)}$ is the second-order Dirac δ function. Nonclassical light corresponds to the states for which the Glauber–Sudarshan P -representation is not positive definite.

A multimode coherent state is a tensor product of single-mode coherent states,

$$|\vec{\alpha}\rangle = \prod_{i=1}^n |\alpha_i\rangle_i, \quad (2.9)$$

where each mode i has dimensionless complex amplitude α_i . A straightforward extension of the single-mode theory given above can then be made to the multimode case. For example, the Glauber–Sudarshan representation is generalized to:

$$\hat{\rho} = \int \prod_{i=1}^n d^2\alpha_i P(\vec{\alpha}) |\vec{\alpha}\rangle \langle\vec{\alpha}|. \quad (2.10)$$

A particularly important case is the weak field. If a coherent field is attenuated to a level at which the probability of detecting more than one photon in the field,

with an ideal unit-efficiency detector, is negligible, then the multimode coherent state (2.9) can be expanded as the normalized state,

$$|\vec{\alpha}\rangle \approx \frac{\prod_{i=1}^n |0\rangle_i + \sum_{i=1}^n \prod_{j=1}^n \alpha_i |\delta_{ij}\rangle_j}{\sqrt{1 + \sum_{i=1}^n |\alpha_i|^2}}, \quad (2.11)$$

where no more than one photon exists in the field. In the single-mode case, the weak coherent field can be expressed as:

$$|\alpha\rangle \approx [1 + |\alpha|^2]^{-1/2} [|0\rangle + \alpha |1\rangle], \quad (2.12)$$

indicating that a coherent superposition exists between the absence of the photon and the presence of the photon in the field mode.

Interference involves the mixing of two fields. With an interferometer constructed with beam splitters, mirrors and passive phase-shifters, the output is a two-mode coherent state which, in the weak-field limit, can be viewed as representing the interference of a photon with itself. This self-interference of a photon has been interpreted as a sum over histories (Feynman, Leighton and Sands [1963]). In this picture, a photon can take either of two separate paths from the source to the detector. Associated with each path is a certain complex probability amplitude a_i ($i = 1, 2$), whose absolute square represents the probability of the photon taking this path. The intensity at the detector is then obtained by summing the probability amplitudes for the two paths and taking the square of its modulus $|a_1 + a_2|^2$, which gives the probability of detecting a photon at this point. Each photon therefore interferes only with itself; it is the basic quantum uncertainty of which path the photon takes through the apparatus that is responsible for the interference effect.

The quantum regime is attained for classical coherent light fields when the time interval between photodetection events, with an ideal, perfectly efficient detector, is much greater than the transit time of radiation through the system. If the state of the radiation field produced by the laser is represented by the coherent state $|\alpha\rangle$, then the attenuated laser field is given by $|\sqrt{\eta}\alpha\rangle$, where $|\alpha|^2$ is the photon flux prior to attenuation, and $\eta|\alpha|^2$ is the photon flux following attenuation. Attenuation does not destroy the coherence of the beam, or affect the coherence time. However, a reduction of the photon flux increases the integration time required to observe coherence effects, and can eliminate the possibility of detecting interference if the integration time required exceeds the coherence time.

2.2. INDEPENDENT SOURCES

To observe interference effects with independent sources, the measurements must occupy a time scale shorter than the mutual coherence time, and the average number of photons received during this time must be large enough to obtain an adequate signal-to-noise ratio.

If two independent laser beams are attenuated to a level where the mean photon number is less than one, the resulting field is brought into the quantum regime and can be regarded as the product of two coherent states corresponding to two independent modes $|\alpha_1\rangle_1$ and $|\alpha_2\rangle_2$. The state of the field is then given by the relation

$$|\alpha_1, \alpha_2\rangle_{1,2} = |\alpha_1\rangle_1 |\alpha_2\rangle_2 \approx \frac{|0\rangle_1 |0\rangle_2 + \alpha_1 |1\rangle_1 |0\rangle_2 + \alpha_2 |0\rangle_1 |1\rangle_2}{\sqrt{1 + |\alpha_1|^2 + |\alpha_2|^2}}. \quad (2.13)$$

The weak two-mode coherent state is therefore a coherent superposition of one photon in mode 1 or one in mode 2, as well as a contribution due to no photon in either mode. If the state represented by eq. (2.13) is conditioned on the detection of a photon, the vacuum state is eliminated from the superposition, yielding the entangled state,

$$|1; 0\rangle_{1,2}^{\theta, \xi} \equiv \cos \theta |1\rangle_1 |0\rangle_2 + e^{i\xi} \sin \theta |0\rangle_1 |1\rangle_2, \quad (2.14)$$

where $\theta = \tan^{-1} |\alpha_2/\alpha_1|$, and $\xi = \arg(\alpha_2/\alpha_1)$.

2.3. TWO-ATOM SOURCES

Laser-driven atoms emit radiation through the process of resonance fluorescence. A case of particular interest is where two identical atoms are made to fluoresce coherently, so that each photon can be regarded as arriving at the detector by a superposition of the paths from the two sources. Vigué, Grangier, Roger and Aspect [1981] and Vigué, Beswick and Broyer [1983] produced two identical atoms travelling in opposite directions by photodissociation of a homonuclear molecule. Time-resolved studies of the fluorescence from such a diatomic source were carried out by Grangier, Aspect and Vigué [1985]. They excited the $X^1\Sigma_g^+$ state of a beam of Ca_2 molecules to the $^1\Pi_u$ dissociative state with a mode-locked pulsed Kr^+ laser beam having a wavelength of 406.7 nm. The fluorescence radiation (wavelength 422.7 nm) was emitted perpendicular to the plane of the atomic beam and the electric field of the Kr^+ laser beam. Time-resolved studies

of the fluorescence revealed a modulation that could be taken as evidence for quantum interference, due to the indistinguishability of the paths from the two sources.

2.4. SOURCES OF NONCLASSICAL LIGHT

With a single-mode laser source, the arrival of photons at a photo detector exhibits a Poisson distribution. With a thermal source, the optical field can be regarded as the sum of the fields contributed by many independent coherent sources. Hence, with classical light sources, such as thermal sources and lasers, photo detections are more likely to occur at the same time, or very close together, than farther apart in time. This phenomenon is known as photon bunching (Mandel and Wolf [1965]) and has been attributed to the fact that photons are bosons. None of these sources can therefore generate any form of nonclassical light, such as a single-photon state.

2.5. SINGLE-PHOTON STATES

The creation of an n -photon state is not easy. One method for preparing an approximation to a single-photon state is by generating a pair of photons. Essentially, the process is one of conditional preparation: given that either two photons exist or no photon exists, the detection of one photon acts as a signal that a second photon is present in the field. The frequency and direction of propagation of the second photon are related to those of the first by conservation laws, and can be determined by analysing the first “gate” photon. The second photon field can then be regarded as being in a one-photon Fock state.

2.5.1. Atomic cascade

Two nearly simultaneous photons can be produced by an atomic cascade (Kocher and Commins [1967], Freedman and Clauser [1972]) using atoms of calcium, which are excited to the 6^1P_1 state by means of a UV source, such as a hydrogen arc lamp. About 10% of these atoms then go into the 6^1S_0 level, from which they return to the ground state *via* the 4^1P_1 level. In this two-step process they emit, in rapid succession, two photons with wavelengths of 551.3 nm and 422.7 nm, respectively. A more efficient procedure is to excite the atoms selectively to the upper level of the cascade by two-photon absorption, using a Kr^+ laser ($\lambda = 406.7$ nm) and a dye laser tuned to resonance for the two-photon process ($\lambda = 581$ nm). The time interval between the emission of the two photons

corresponds to the lifetime ($\tau_s = 4.7$ ns) of the intermediate state of the cascade (Aspect, Grangier and Roger [1981]).

2.5.2. Parametric down-conversion

The atomic cascade suffers from two drawbacks: the emission of the two photons is not perfectly simultaneous, and the correlation between their directions is not perfect. Parametric down-conversion overcomes these problems. In this process, a single UV photon decays spontaneously in a crystal with a $\chi^{(2)}$ nonlinearity into two photons (a *signal* photon and an *idler* photon) with wavelengths close to twice the UV wavelength (Harris, Oshman and Byer [1967], Klyshko [1967], Burnham and Weinberg [1970]). Down-conversion is facilitated by using a birefringent crystal to achieve phase matching. The two down-converted photons are highly correlated and are emitted with a negligible time separation (Hong and Mandel [1985], Friberg, Hong and Mandel [1985]). Since energy is conserved in the process, we have:

$$\hbar\omega_0 = \hbar\omega_1 + \hbar\omega_2, \quad (2.15)$$

where $\hbar\omega_0$ is the energy of the UV photon, and $\hbar\omega_1$ and $\hbar\omega_2$ are the energies of the two down-converted photons. Similarly, since momentum is conserved, we have:

$$\mathbf{k}_0 = \mathbf{k}_1 + \mathbf{k}_2, \quad (2.16)$$

where \mathbf{k}_0 is the momentum of the UV photon, and \mathbf{k}_1 and \mathbf{k}_2 are the momenta of the down-converted photons. It follows from eq. (2.15) that, while the frequencies of the individual down-converted photons may vary over a broad range, the sum of their frequencies is well defined. Similarly, it follows from eq. (2.16) that the photons in each pair are emitted on opposite sides of two cones, whose axis is the UV beam, and produce, as shown in fig. 2.1, a set of rainbow colored rings.

In a typical realization, Hong and Mandel [1986] used the UV beam from an argon-ion laser ($\lambda = 351.1$ nm) and a potassium dihydrogen phosphate (KDP) crystal to generate pairs of photons with wavelengths around 746 and 659 nm. These photons leave the crystal at angles of approximately $\pm 1.5^\circ$ to the UV beam.

2.6. THE BEAM SPLITTER

Adam, Janossy and Varga [1955a,b] were the first to study the correlations between photons at a beam splitter, rather than the amplitude correlations

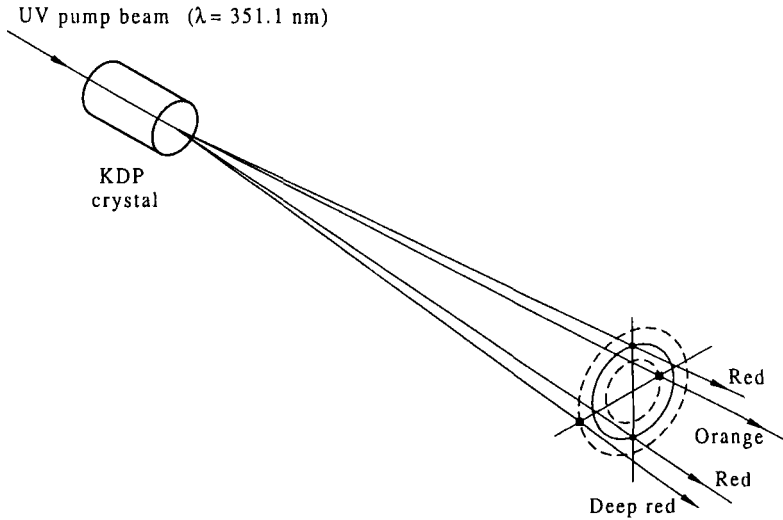


Fig. 2.1. Generation of photon pairs by parametric down-conversion of UV photons in a nonlinear crystal. Conjugate photons are emitted on opposite sides of the UV beam; typically, one photon has a slightly lower frequency than the other.

measured by normal interferometric techniques. Subsequently, Hanbury Brown and Twiss [1956] (see also Hanbury Brown [1974]) measured photon correlations in thermal light fields in their experiments leading to the intensity interferometer (see § 5), while Arecchi, Berné and Burlamacchi [1966] studied photon correlations with laser sources. For a thermal source, the correlation between photons detected at the two outputs of a beam splitter is positive; for a coherent field from a laser, there is no correlation between the two outputs.

On the other hand, nonclassical fields with definite photon number exhibit a very different behavior. With a single-photon state, quantum mechanics predicts a perfect anticorrelation between the counts at the two output ports of a beam splitter (Clauser [1974]). Grangier, Roger and Aspect [1986], as well as Diedrich and Walther [1987], observed such anticorrelations, indicating that each photon was either transmitted or reflected. The perfect anticorrelation of photons at the beam splitter can be regarded as evidence of the indivisibility of the photon.

The indivisibility of the photon provides the simplest example of entanglement. The output from the beam splitter can be regarded as the superposition of two histories, the first consisting of one photon at port 1 and no photon at port 2, and the second consisting of no photon at port 1 and one photon at port 2. This superposition state cannot be reduced because of the strong anticorrelation

of the two modes that arises from the entanglement of the input field with the vacuum field represented by eq. (2.14).

It follows that any analysis of the effect of a beam splitter on an incident beam of light with definite photon number has to take into account the vacuum field at the unused input port (Fearn and Loudon [1987, 1989], Campos, Saleh and Teich [1989]). Such a treatment confirms the effects observed with classical fields as well as with photon-number states. When one of the input photon-number states is the vacuum and the other is a nonzero number state, the photon numbers at the output ports are described by a binomial distribution (Brendel, Schürtrumpf, Lange, Martienssen and Scully [1988]). However, if the inputs at the two ports of a 50:50 beam splitter are identical single-photon states, the joint probability for detecting a photon at each of the two output ports vanishes. This implies that both incident photons must exit together at either of the two output ports, and is an example of quantum-mechanical interference of the probability amplitudes for a photon pair (Hong, Ou and Mandel [1987]).

2.7. SQUEEZED STATES OF LIGHT

The coherent state $|\alpha\rangle$ incorporates vacuum fluctuations which become observable with phase-sensitive detection schemes, such as heterodyne or homodyne detection. These vacuum fluctuations are responsible for the limit on the accuracy of measurements set by shot noise, known as the standard quantum limit (SQL). Yuen [1976] performed a detailed analysis of what he then called *two-photon coherent states* which revealed the possibility of reducing quantum noise using such states.

We can represent the electric field of a monochromatic light wave as the sum of two quadrature components in the form:

$$E = E_0 [X_1 \cos \omega t + X_2 \sin \omega t], \quad (2.17)$$

where X_1 and X_2 are complementary operators satisfying the commutation relation $[X_1, X_2] = \frac{1}{2}i$, whose variances therefore obey the uncertainty relationship

$$\Delta X_1 \Delta X_2 \geq \frac{1}{4}. \quad (2.18)$$

For normal coherent light the variances are equal. For a squeezed state the variances are unequal, although their product remains unchanged. Accordingly, it is possible to reduce phase fluctuations with squeezed light, as shown in fig. 2.2, at the expense of a corresponding increase in the amplitude fluctuations (Caves [1981], Walls [1983]).

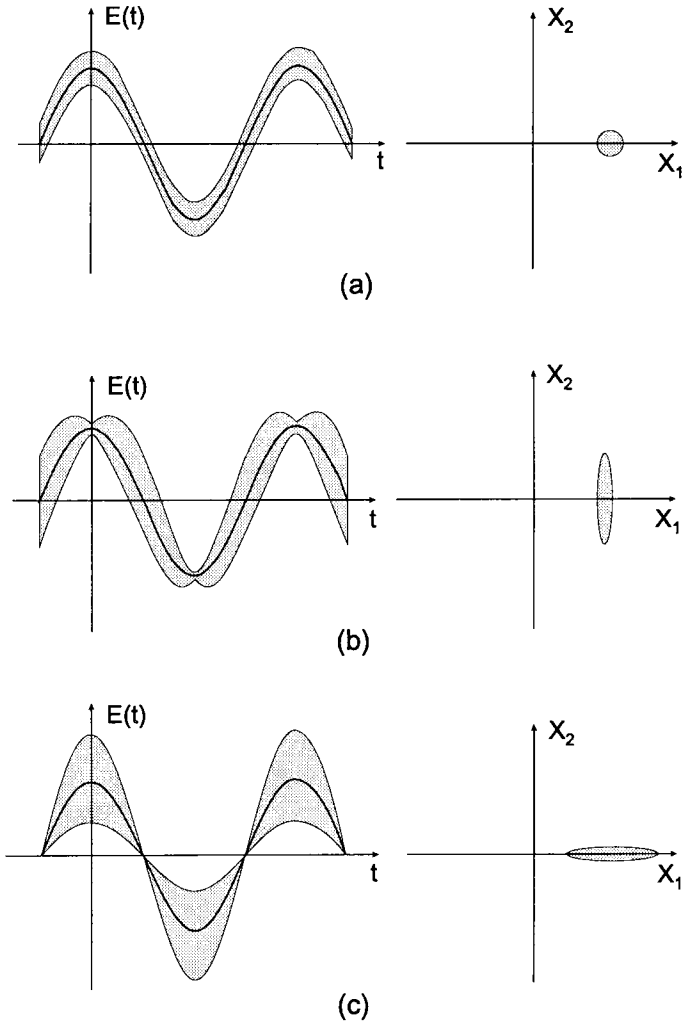


Fig. 2.2. Plot of electric field against time, showing the uncertainty for (a) a coherent state, (b) a squeezed state with reduced amplitude fluctuations, and (c) a squeezed state with reduced phase fluctuations (Caves [1981]).

The degree of squeezing can be measured with a balanced homodyne detector, which yields a phase-sensitive measurement of the noise. As shown in fig. 2.3, the squeezed light is combined with another strong beam from the same source, which constitutes a local oscillator, at a 50:50 beam splitter. The beams emerging from the beam splitter are directed to two photo detectors, and the difference of

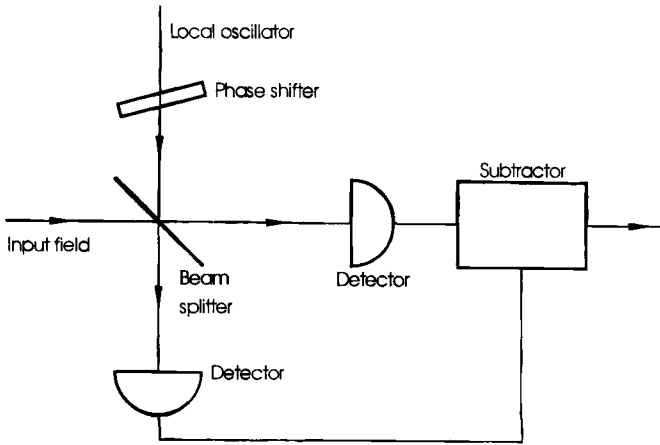


Fig. 2.3. Balanced homodyne detector used for measurements of noise due to a single field-quadrature component.

the two photocurrents is displayed. With this arrangement, intensity fluctuations in the local oscillator and the signal cancel out, and the output corresponds to the interference of the local oscillator with the signal. If the intensity of the local oscillator is much greater than that of the signal, the fluctuations in the output are essentially due to the signal. As the phase difference between the squeezed light signal and the local oscillator is varied, the detector becomes sensitive first to one quadrature amplitude and then to the other, and the output noise amplitude varies accordingly.

The concept of single-mode squeezed states can be extended to two or more correlated modes. Milburn [1984] and Caves and Schumaker [1985] considered two-mode states consisting of a two-mode coherent field with squeezed vacuum fluctuations. Whereas the single-mode squeezed state is generated by photon-pair creation and annihilation in one mode, the two-mode squeezed state is generated by photon-pair creation and annihilation in two modes. The two photons in the pair, each with a different frequency, are strongly correlated, and this correlation is responsible for the squeezed fluctuations.

The process of generating photon pairs is not restricted to parametric down-conversion and can be implemented with any order of nonlinearity. A number of physical phenomena can therefore be used, in principle, to generate squeezed states. The earliest and most common method has been degenerate four-wave mixing in a medium with a nonlinear susceptibility (Slusher, Hollberg, Yurke, Mertz and Valley [1985], Shelby, Levenson, Perlmutter, de Voe and Walls [1986], Maeda, Kumar and Shapiro [1987]). In such a process, energy is transferred

from two strong pump beams to two weaker beams. As a result, correlations are established between the photons in the two weaker beams. When these two beams are combined, the resulting light exhibits the characteristics of squeezed states. A greater reduction in noise has been achieved by degenerate parametric down-conversion (Wu, Kimble, Hall and Wu [1986]). When the gain from parametric amplification becomes large in the down-conversion crystal, there is a transition from spontaneous to stimulated emission. Since the gain depends on the phase of the amplified light relative to the phase of the pump beam, vacuum fluctuations in one quadrature are squeezed (Kimble and Walls [1987]).

§ 3. Second-order Interference

The apparent contradiction between viewing light as particles and light as waves provided the impetus for studying the interference of a light beam with itself at power levels so low that the probability of two or more photons existing at the same time within the apparatus was negligible. If light is thought of as particles, and interference is a phenomenon involving the interaction of at least two particles, classical considerations suggest that interference effects should become weaker as the number of photons decreases and disappear completely when no more than one photon is in the apparatus at a time.

3.1. INTERFERENCE AT THE "SINGLE-PHOTON" LEVEL

These considerations led to a series of experiments involving photographic recordings of interference patterns at extremely low light levels, all of which showed that the quality of the pattern did not depend on the intensity (Taylor [1909], Gans and Miguez [1917], Zeeman [1925], Dempster and Batho [1927]). This result was also confirmed by counting photons with a photomultiplier (Janossy and Naray [1957]). A detailed review of these experiments involving interferometry at low light levels has been presented by Pipkin [1978].

While these experiments supported the predictions of quantum theory, all of them used conventional thermal light sources. The light from such a thermal source can be modeled as an ensemble of coherent states, each of which can be described by a classical electromagnetic field, even when it is highly attenuated. Accordingly, it could be argued that these experiments did not actually involve single-photon states.

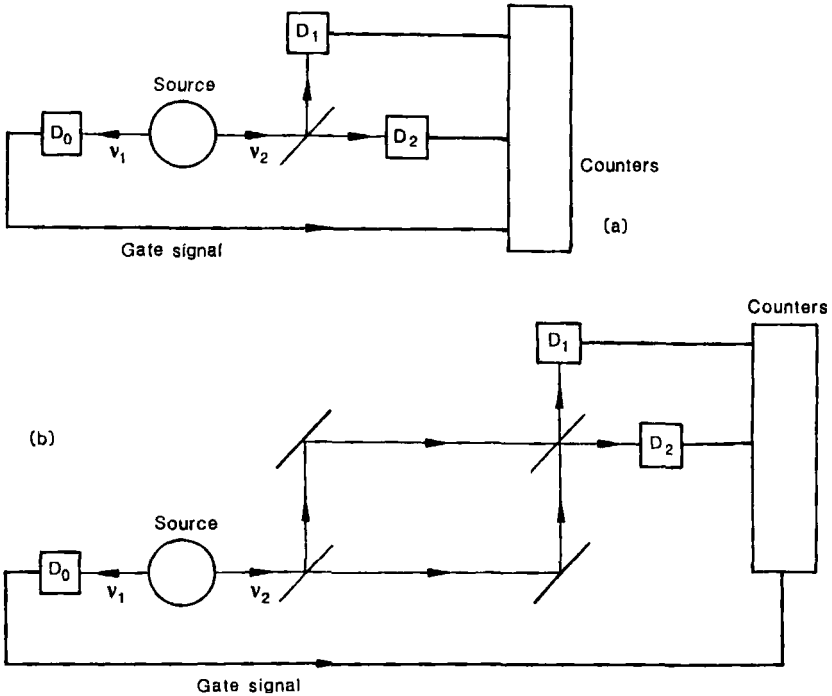


Fig. 3.1. Experimental arrangement used (a) to detect single-photon states and (b) to demonstrate interference with single-photon states (Grangier, Roger and Aspect [1986]).

3.2. INTERFERENCE WITH SINGLE-PHOTON STATES

Interference effects produced by light without a positive definite Glauber–Sudarshan P -representation cannot be explained in classical terms. A good example is interference with single-photon states, which was first studied using an atomic cascade (see § 2.5.1) by Grangier, Roger and Aspect [1986], and also by Aspect and Grangier [1987].

As shown in fig. 3.1a, the arrival of the first photon (frequency ν_1) at the detector D_0 acted as a trigger for a gate generator, enabling the two detectors D_1 and D_2 on the two sides of the beam splitter for a time $2\tau_s$. During this period, the probability for the detection of a second photon (frequency ν_2) emitted by the same atom is much greater than the probability of detecting a similar photon emitted by any other atom in the source.

While a classical wave would be divided between the two output ports of the beam splitter, a single photon cannot be divided in this fashion. We can therefore

expect an anticorrelation between the counts on the two sides of the beam splitter at D_1 and D_2 , measured by a parameter

$$\mathcal{A} \equiv \frac{N_{012}N_0}{N_{01}N_{02}}, \quad (3.1)$$

where N_{012} is the rate of triple coincidences between the detectors D_0 , D_1 and D_2 ; N_{01} and N_{02} are the rate of double coincidences between D_0 and D_1 and D_0 and D_2 , respectively, and N_0 is the rate of counts of D_0 . For a classical wave, it follows from Schwarz's inequality that $\mathcal{A} \geq 1$, while the indivisibility of the photon should lead to arbitrarily small values of \mathcal{A} . As expected, the number of coincidences observed for the second photon, with a gate time of 9 ns, was only 0.18 of that expected from classical theory, but corresponded to that predicted by quantum theory. This source was then used in the optical arrangement shown in fig. 3.1b, with the detectors D_1 and D_2 receiving the two outputs from a Mach-Zehnder interferometer. The interferometer was initially adjusted and checked without the gating system in operation, and interference fringes with a visibility $\mathcal{V} > 0.98$ were obtained. In the actual experiment, with the gate on, the optical path difference was varied around zero in 256 steps, each of $\lambda/50$, with a counting time of 1 s at each step. The results of 15 such sweeps were then averaged to improve the signal-to-noise ratio. Analysis of the data showed that, even with the gate operating, values of the visibility $\mathcal{V} > 0.98$ were obtained.

The results of these experiments confirmed the predictions of quantum mechanics and Dirac's view that the photon interferes with itself. The self-interference of a photon can be understood, as discussed in § 2.1, through Feynman's concept of a sum over histories (Feynman, Leighton and Sands [1963]).

3.3. INTERFERENCE WITH INDEPENDENT SOURCES

Problems appear with Dirac's dictum when we consider interference effects produced by light beams from two completely independent sources (Magyar and Mandel [1963], Paul [1986]). Two independent waves can produce an interference pattern, provided that the phase difference between the waves is stable over the observation period. In the photon picture, however, the question is: "How can an interference pattern be produced if the photons in the two beams are created independently?" Since the photon that is detected does not always originate from the same source, the picture of a single photon being created and propagated along a superposition of two distinct paths no longer holds.

The first experiments demonstrating interference between two independent laser beams at very low light levels were performed by Pfleeger and Mandel

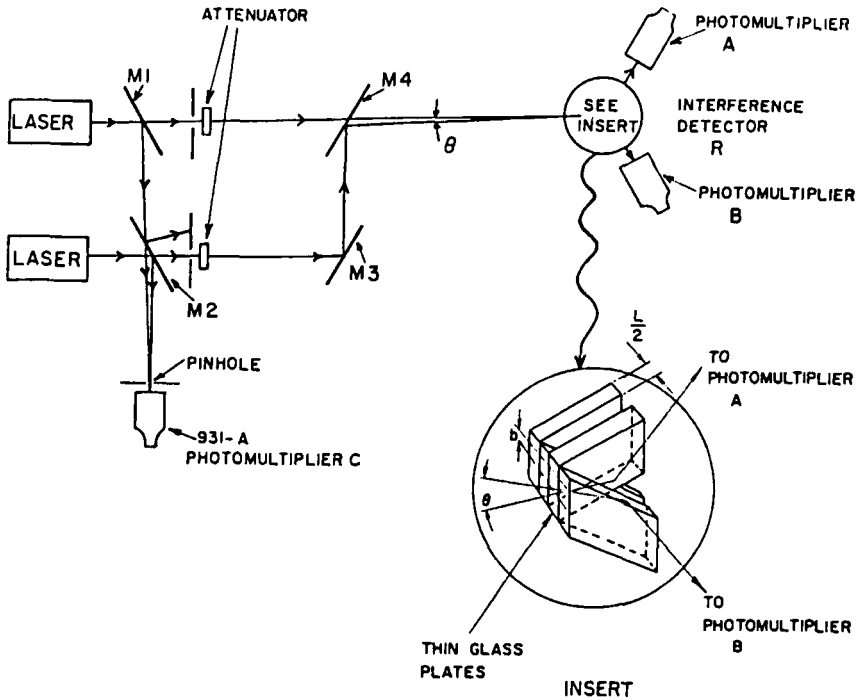


Fig. 3.2. Experimental system used to demonstrate interference with two independent laser sources (Pfleeger and Mandel [1968]).

[1967a,b, 1968]. As shown in fig. 3.2, the light beams from two independent He-Ne lasers were superimposed at a small angle to produce interference fringes on the edges of a stack of glass plates whose thickness was equal to half the fringe spacing. Two photomultipliers received the light from alternate plates, so that when interference fringes were present, a negative correlation was obtained between the number of counts registered by the photomultipliers. To minimize effects due to movements of the fringes, an additional photo detector was used to detect beats between the beams, and observations were restricted to $20\ \mu\text{s}$ intervals, corresponding to periods during which the frequency difference between the two laser beams was less than $30\ \text{kHz}$. The transit time was approximately $3\ \text{ns}$, while the photon fluxes in the two beams were around 3×10^6 photons/s and the quantum efficiency of the photomultipliers was about 0.07, so that about 10 photons were detected in each $20\ \mu\text{s}$ period. The average of 400 such measurements was taken in each experiment.

In this experiment, the positions of the fringe maxima are not predictable

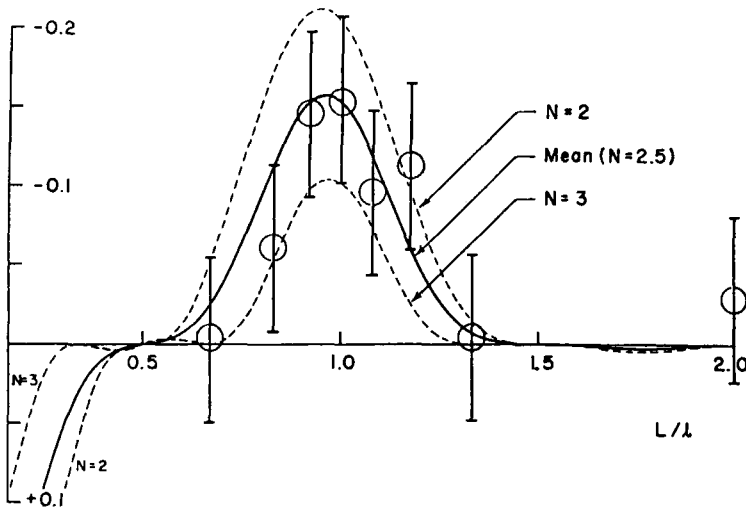


Fig. 3.3. Experimental results for the normalized correlation coefficient, together with the theoretical curves for $N=2$ and $N=3$ (Pfleeger and Mandel [1968]).

and vary from measurement to measurement. However, there should always be a negative correlation between the number of photons registered in the two channels, which should be a maximum when the fringe spacing l is equal to L , the thickness of a pair of plates. Figure 3.3 shows the variation in the degree of correlation of the two counts with the ratio L/l , together with the theoretical curves for $N=2$ and $N=3$, where N is the number of pairs of plates in the detector array. In subsequent experiments, the measurement procedure was automated, making it possible to record a much larger number of counts in each run, and to investigate the effects of varying the observation time and the number of interference fringes sampled.

Similar results were also obtained by Vain'shtein, Melekhin, Mishin and Podolyak [1981], in observations on the transient interference patterns formed by the beams from two lasers with two photomultipliers operating in the photon-counting regime.

These experiments confirmed that interference effects were associated with the detection of each photon, but their statistical accuracy was limited by the fact that observations could be made only over very short time intervals, during which a very small number of photons was detected. This problem has been overcome in more recent experiments involving observations of interference effects in the time domain.

3.4. INTERFERENCE IN THE TIME DOMAIN

Interference effects between two independent light sources were first observed in the time domain by Forrester, Gudmundsen and Johnson [1955], who mixed the Zeeman components of a visible spectral line at a fast photo detector. Subsequently, Javan, Ballik and Bond [1962] showed that beats could be obtained by superimposing the beams from two independent He-Ne lasers, or the beams corresponding to two axial modes of the same laser, at a photo detector. Observations on such beats have been used successfully to study interference effects with two sources at very low light levels (Hariharan, Brown and Sanders [1993]).

For such observations, there are significant advantages in using the beat produced by two axial modes of the same laser, since the frequency variations of the two modes due to thermal effects and mechanical variations of the cavity length are very nearly the same. A convenient low beat frequency can be obtained by applying a transverse magnetic field to a He-Ne laser that is oscillating in two longitudinal modes. The laser then oscillates on a single axial cavity mode composed of two orthogonally polarized components which exhibit a small frequency difference due to the magnetically induced birefringence of the gas in the laser tube (Morris, Ferguson and Warniak [1975]). These two Zeeman-split components can be regarded as equivalent to beams from two independent lasers, because the coupling between them is quite weak. In addition, with normal excitation, there is no coherence between the two upper states for the lasing transitions.

The experimental arrangement is shown schematically in fig. 3.4. The beat frequency was stabilized by mixing the two orthogonally polarized components in the back beam of the laser, with a polarizer, at a monitor photo diode and feeding the output to a frequency-to-voltage converter, which controlled the length of the cavity through a servo amplifier and a heating coil on the laser tube (Ferguson and Morris [1978]). A beat frequency of 80 kHz, with a frequency bandwidth estimated at 1 Hz, was obtained.

To make measurements, a set of neutral density filters was used to reduce the intensity of the output beams from the laser in accurately known steps over a range of $10^8:1$. The attenuated beams were incident, after passage through a polarizing prism that brought them into a condition to interfere, on a photo diode. The signal from this photo diode was taken through a band-pass filter to a homodyne detector that was fed with a reference signal from the monitor photo diode. Because the variations in the frequency of the beat signal were small and were tracked by the reference signal from the monitor photo diode,

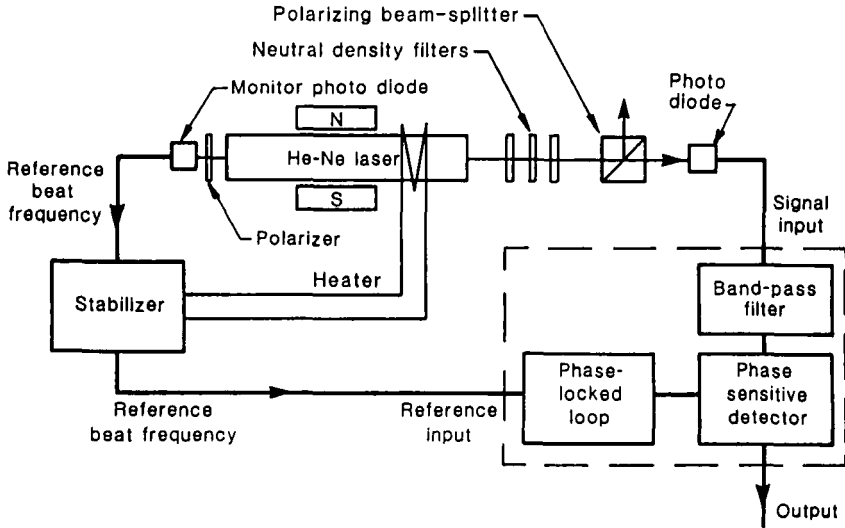


Fig. 3.4. Experimental system used to measure the amplitude of the beats produced by the two orthogonally polarized modes from a transverse Zeeman laser at very low light levels (Hariharan, Brown and Sanders [1993]).

measurements could be made with integrating times up to 100 seconds to obtain a good signal-to-noise ratio even at the lowest light levels.

Observations were made with the photo diode at a distance of 0.2 m from the laser, as the incident power was varied from $1.0\ \mu\text{W}$ down to $4.8\ \text{pW}$, corresponding to values of the incident flux ranging from 3.18×10^{12} photons/s to 1.53×10^7 photons/s, respectively. At the lowest power level, the probability for the presence of more than one photon in the apparatus at any time, relative to that for the presence of a single photon, was less than 0.005.

Figure 3.5 shows the output from the homodyne detector plotted as a function of the power incident on the photo diode. The measurements showed no significant deviations from a straight line with a slope of unity, confirming that the interference phenomena remained unchanged down to power levels at which there was a very high probability that one photon was absorbed before the next one was generated.

These results were extended to cover interference involving more than two beams by Hariharan, Brown, Fujima and Sanders [1993] using a He-Ne laser operating in three axial modes. With such a laser, low-frequency beat signals are also obtained because the axial modes are not equally separated in frequency, due to the dispersion of the excited neon gas. The frequency of these beats

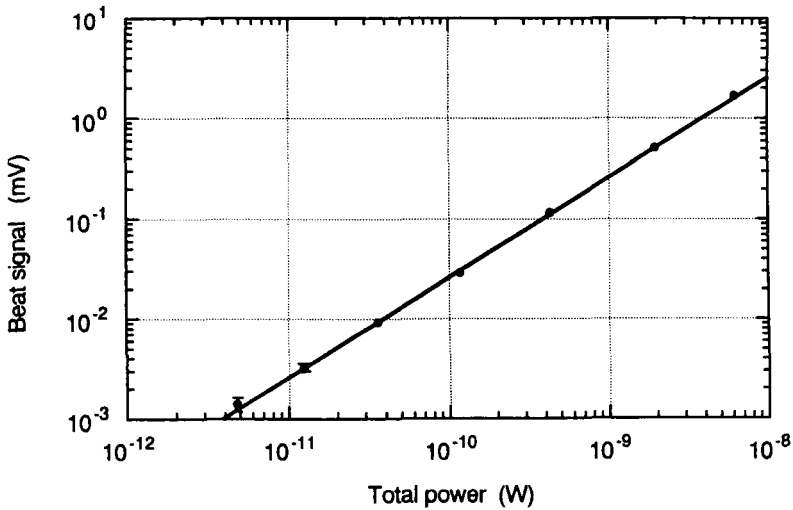


Fig. 3.5. Output signal from the homodyne detector as a function of the total power of the laser beams (Hariharan, Brown and Sanders [1993]).

corresponds to the second differences between the frequencies of the modes (Casabella and Gonsiorowski [1980]).

In the actual experiment, the photo detector was placed at a distance of 80 mm from the neutral density filters used to attenuate the beam. Measurements were made of the output from the homodyne detector as the power incident on the photo diode was varied from 75 nW down to 0.19 nW, corresponding to values of the flux ranging from 2.39×10^{11} photons/s to 6.04×10^8 photons/s. At the lowest power level, the ratio of the probability for the presence of at least one photon from all three modes to the total probability for the presence of at least one photon from any mode, was only 0.0009. However, the amplitude of the low-frequency beat was found to vary linearly with the power incident on the photo diode down to this power level.

These results also showed that the ratio of the beat amplitude to the incident power remained unchanged down to the lowest power level at which observations were made, even though, at this power level, the mean time interval between the arrival of successive photons at the photo detector was greater than the period of the beat (Hariharan, Brown, Fujima and Sanders [1995]).

3.5. SUPERPOSITION STATES

It follows that the interference phenomena observed in all these cases are

associated with the detection of each photon and not with the interference of one photon with another. An analysis of the processes leading to interference effects made by Jordan and Ghilmetti [1964] and by Mandel [1964] suggested that for interference effects to become observable, the average number of photons in the same spin state falling on a coherence area in a coherence time, or the average occupation number per unit cell of phase space, would have to be appreciably greater than 1. An alternative explanation by de Broglie [1969] involved the assumption that the distribution of photons was determined by the superposition of weak electromagnetic waves from the two sources. However, it is now clear that the interference phenomena are produced by a sequence of photons, each one of which is in a superposition state that originates from the modes involved. The problem that remains is how the superposition state responsible for interference arises.

One explanation is that the superposition state is produced in the process of absorption at the photodetector, because it is impossible, in principle, to determine from which source the photon is emitted. The measurement therefore forces the photon into a superposition state in which it behaves as if it were associated with both light beams, and these two states of each photon interfere (Mandel [1976]). A field-theoretic analysis explaining how this happens has been presented by Walls [1977]. Alternatively, it is possible to regard the fields from each source as being in a superposition state of having one photon and no photon (Hariharan, Brown and Sanders [1993]). An explicit description of the interference effects produced by two independent laser beams using the techniques of quantum field theory has also been presented by Agarwal and Hariharan [1993].

§ 4. The Geometric Phase

An extension of the adiabatic theorem of quantum mechanics by Berry [1984] showed that the wave function of a quantum system may undergo a phase shift (a geometric phase) when the parameters of the system undergo a cyclic change. This phase change can be observed by interference if the cycled system is compared with another system that has not undergone any change.

4.1. THE GEOMETRIC PHASE IN OPTICS

Demonstrations of effects due to the geometric phase in optics followed. One example was the rotation of the plane of polarization of a linearly polarized

light beam propagating in an optical fiber coiled into a helix (Tomita and Chiao [1986]). Another was the phase shift observed in a Mach–Zehnder interferometer in which the two beams traversed nonplanar paths arranged to have equal lengths, but opposite senses of handedness (Chiao, Antaramian, Ganga, Jiao, Wilkinson and Nathel [1988]).

Berry's paper also led to a reappraisal of earlier studies by Pancharatnam [1956] on the interference of polarized light, which could now be seen as manifestations of the geometric phase (Ramaseshan and Nityananda [1986], Berry [1987]).

Pancharatnam defined the phase difference between two beams in different states of polarization by considering the intensity produced when the two beams were made to interfere. He regarded the two beams as being “in phase” when the resultant intensity was a maximum. This approach made it possible to define how a beam changed its phase when its state of polarization was altered. It also led to the observation that a beam could be taken from one polarization state, without introducing any phase changes, through two other polarization states back to its original state, and exhibit a phase shift. The magnitude of this phase shift (the Pancharatnam phase) was equal to half the solid angle subtended by the circuit at the center of the Poincaré sphere. Several experiments have been described using interferometric techniques to measure this phase shift (Bhandari and Samuel [1988], Simon, Kimble and Sudarshan [1988], Chyba, Wang, Mandel and Simon [1988]).

4.2. OBSERVATIONS AT THE SINGLE-PHOTON LEVEL

Observations of the Pancharatnam phase have been made by Hariharan, Roy, Robinson and O'Byrne [1993] at light levels low enough to ensure that the probability of more than one photon being present simultaneously in the interferometer was negligible. They used a Sagnac interferometer in which the optical paths traversed by the two beams were always equal, and a phase difference could be introduced between them only by operating on the Pancharatnam phase. As shown in fig. 4.1, light from a He–Ne laser, linearly polarized at 45° to the plane of the figure by a polarizer P_1 , was divided at a polarizing beam-splitter into two orthogonally polarized beams traversing the same closed triangular path in opposite directions. A second polarizer P_2 , with its axis at 45° to the plane of the figure, brought the two beams leaving the interferometer into a condition to interfere at a photomultiplier. The phase difference between the beams was varied by a system consisting of a rotating

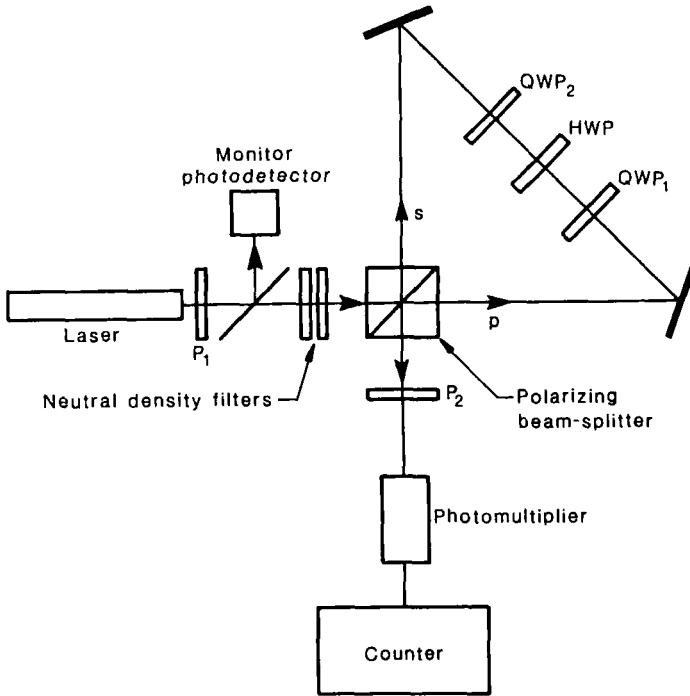


Fig. 4.1. Schematic of the experimental arrangement used for studies of the Pancharatnam phase at the single-photon level (Hariharan, Roy, Robinson and O'Byrne [1993]).

half-wave plate, HWP, located between two fixed quarter-wave plates, QWP_1 and QWP_2 (Hariharan and Roy [1992]).

The operation of this interferometer can be followed by means of the Poincaré sphere (Jerrard [1954]). Light (p-polarized) transmitted by the polarizing beam splitter, passes through the quarter-wave plate QWP_1 , the half-wave plate HWP, and the quarter-wave plate QWP_2 , in that order. As shown in fig. 4.2, the polarization state of this beam then traces out the path $A_1SA_2NA_1$ on the Poincaré sphere. If the half-wave plate HWP is set with its optic axis at an angle $+\theta$ to the optic axes of QWP_1 and QWP_2 , the phase of the transmitted light is advanced by 2θ . Reflected (s-polarized) light traverses the interferometer in the opposite sense, and its polarization state traces out the path $B_1SB_2NB_1$ on the Poincaré sphere; its phase is therefore retarded by 2θ . These operations lead to a phase difference $\Delta\phi = 4\theta$ between the two fields when they reach the photomultiplier, without introducing any change in the optical paths.

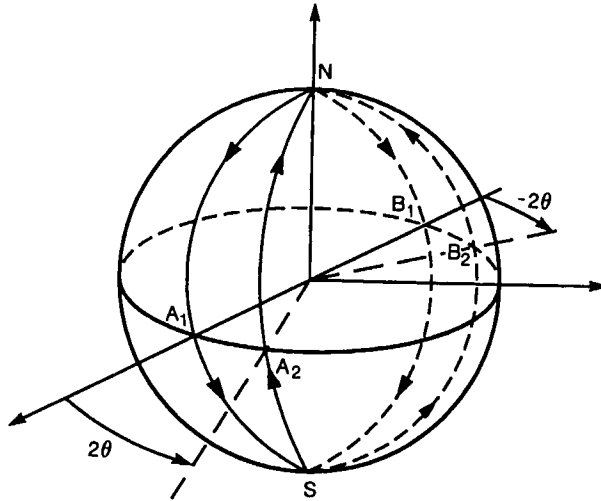


Fig. 4.2. Closed paths traversed by the polarization states of the two beams in the interferometer on the Poincaré sphere (Hariharan, Roy, Robinson and O'Byrne [1993]).

Measurements were made at an input power level < 1 pW, corresponding to a photon flux $N_i < 3.2 \times 10^6$ photons/s, at which level

$$\frac{P(n > 1)}{P(1)} = 0.005, \quad (4.1)$$

where $P(1)$ and $P(n > 1)$ are, respectively, the probabilities for the presence of one photon and more than one photon in the apparatus.

The net counting rate, after subtracting the dark counting rate, exhibited the expected sinusoidal variation, corresponding to the relation $\Delta\phi = 4\theta$, over a wide range of values of θ . The visibility of the interference fringes was better than 0.97 and very close to that obtained in the classical regime.

4.3. OBSERVATIONS WITH SINGLE-PHOTON STATES

An experiment to demonstrate the existence of a geometric phase for single photons was performed by Kwiat and Chiao [1991]. They used a light source that produced pairs of photons with wavelengths centered at 702.2 nm by parametric down-conversion (see § 2.5.2). In the arrangement used by them (see fig. 4.3), the idler beam was transmitted through the filter F1 to the detector D1, while the signal beam entered a Michelson interferometer. The beam leaving the interferometer was incident on a second beam splitter B2, from which it was

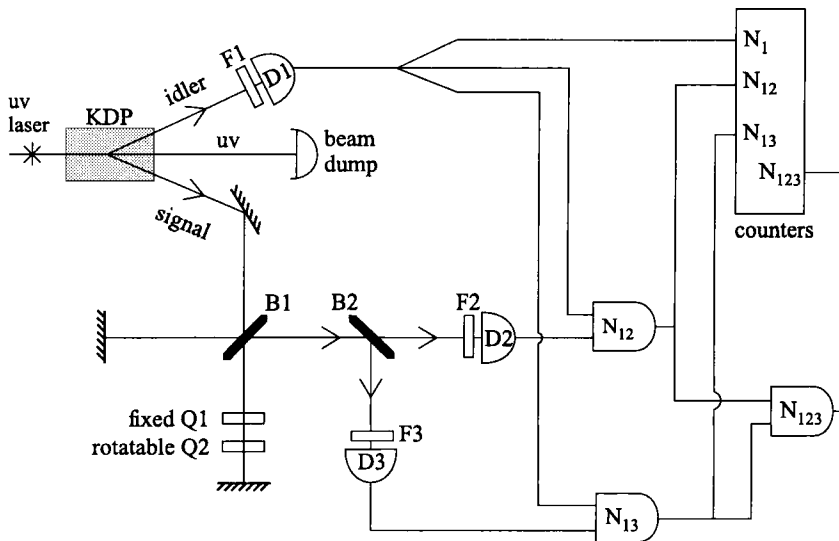


Fig. 4.3. Apparatus used to measure Berry's phase for single photons (Kwiat and Chiao [1991]).

transmitted to the detector D2 through the filter F2 or reflected to the detector D3 through the filter F3. The count rates for coincidences between D1 and D2 and between D1 and D3, as well as triple coincidences between D1, D2 and D3, were recorded.

One arm of the interferometer contained a fixed quarter-wave plate Q1, with its axis at 45° , as well as a quarter-wave plate Q2 that could be rotated. Since the beam traverses this system twice, a rotation of Q2 through an angle θ introduces an additional phase shift in this arm, $\Delta\phi = 2\theta$.

Data were recorded using filters with a bandwidth of 10 nm at F2 and F3, and an optical path difference of $220\ \mu\text{m}$, which is greater than the coherence length corresponding to this bandwidth (about $50\ \mu\text{m}$). As a result, the fringe visibility seen by the detectors D2 and D3, operating individually, was essentially zero. However, when a filter with a bandwidth of 0.86 nm was placed in front of D1, the count rate for coincidences between D1 and D3 varied with the angular setting θ of Q2, as shown in the lower part of fig. 4.4, with a visibility of 0.60 ± 0.05 . With a broad band filter at F1, the coincidence fringes disappeared, as shown in the upper part of fig. 4.4.

With this arrangement, it was possible to verify that the signal beam

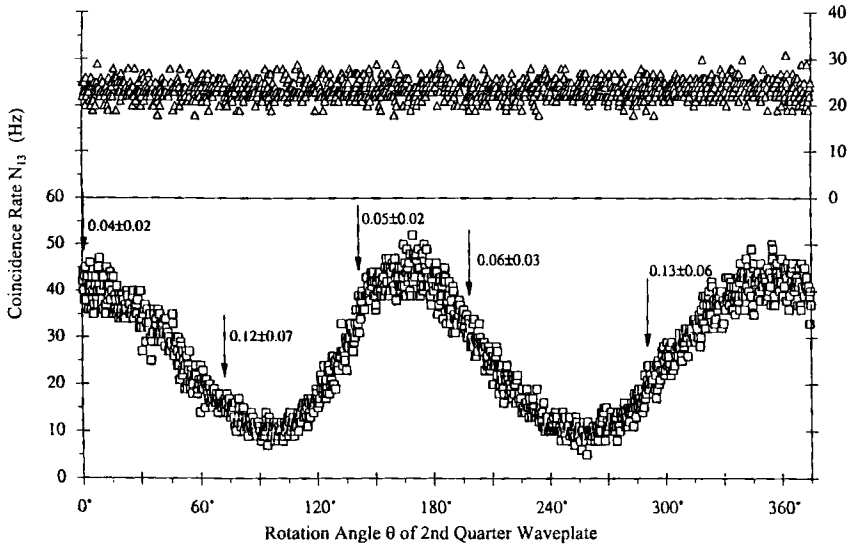


Fig. 4.4. Interference effects (lower trace, squares) with a slowly varying Berry's phase, observed as coincidences between D3 and D1, with an optical path difference of $220\mu\text{m}$ in the interferometer and a narrow band filter at F1. With a broad-band filter at F1, no interference is seen (upper trace, triangles) (Kwiat and Chiao [1991]).

was composed of photons in an $n=1$ Fock state by measurements of the anticorrelation parameter (see § 3.2):

$$\mathcal{A} \equiv \frac{N_{123}N_1}{N_{12}N_{13}}, \quad (4.2)$$

where N_{123} is the rate of triple coincidences between D1, D2 and D3, N_1 is the rate of single counts by D1 alone, N_{12} is the rate of coincidences between D1 and D2, and N_{13} is the rate of coincidences between D1 and D3. The average value of \mathcal{A} obtained with the two-photon source differed from that obtained with a thermal source by more than 13 standard deviations, confirming that the observations essentially involved photons in $n=1$ Fock states.

These observations suggest that the geometric phase observed in optics originates at the quantum level, but survives the correspondence principle limit into the classical level, although this question is still open to argument (Tiwari [1992]).

§ 5. Fourth-order Interference

Measurements of fourth-order coherence can be realized by using two spatially

separated detectors, or by correlating photo detections which are separated in time.

Studies of fourth-order coherence began with the intensity interferometer (Hanbury Brown and Twiss [1956], Hanbury Brown [1974]). In this instrument, light from a star was focused on two photo detectors whose separation could be varied, and the correlation between the fluctuations in the output currents from the two detectors was measured.

The fluctuations in the output current from each detector then consist of two components. One is the shot noise associated with the current, while the other is due to fluctuations in the intensity of the incident light. The shot noise from the two detectors is not correlated, but the intensity fluctuations exhibit a correlation which depends on the degree of coherence of the fields at the two detectors. Since the fields are produced by a stationary thermal source, the normalized intensity correlation function depends only on the time difference, τ , and is given by the relation

$$\mathcal{R}(\mathbf{r}_1, \mathbf{r}_2, \tau) = |\gamma^{(1,1)}(\mathbf{r}_1, \mathbf{r}_2, \tau)|^2, \quad (5.1)$$

where $\gamma^{(1,1)}(\mathbf{r}_1, \mathbf{r}_2, \tau)$ is the normalized second-order coherence function. When $\tau = 0$, the variation of the normalized value of the correlation with the separation of the detectors can be used to determine the angular diameter of a star. With a time delay τ produced by an optical path difference that is much greater than the coherence length of the radiation, the effects of such correlated intensity fluctuations can be observed as a spectral modulation (Alford and Gold [1958], Mandel [1962]).

5.1. NONCLASSICAL FOURTH-ORDER INTERFERENCE

Fourth-order interference provides a means for distinguishing classical and nonclassical light, since an optical field can exhibit nonclassical fourth-order interference effects even when the usual second-order interference effects cannot be observed (Mandel [1983], Ou [1988]). Such fourth-order interference effects can be observed with correlated photons produced by parametric down-conversion (Ghosh, Hong, Ou and Mandel [1986], Ghosh and Mandel [1987]).

We consider the detection of the field produced by the signal and idler modes from a two-photon source at a point x_1 (see fig. 5.1). Since the output from the down-converter is an approximation to the two-photon Fock state $|1, 1\rangle_{AB}$ for

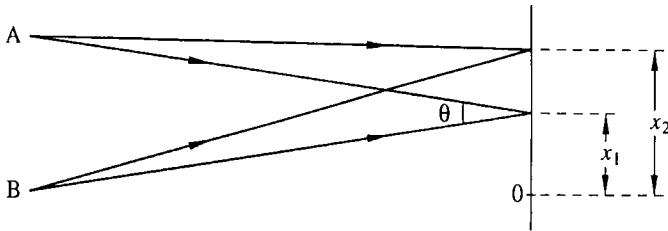


Fig. 5.1. Geometry of a fourth-order interference experiment (Ghosh and Mandel [1987]).

weak fields, the probability of detecting a photon between the arbitrary positions x_1 and $x_1 + \delta x_1$ can be shown to be:

$$\mathcal{P}_1(x_1) \delta x_1 = 2K_1 \delta x_1, \quad (5.2)$$

where K_1 is a scale factor. This probability is independent of x_1 , so that no interference fringes can be seen. A separate measurement made at x_2 with another photo detector yields a similar result. The reason for the absence of second-order interference is, of course, that no definite phase relationship exists between the two down-converted fields.

However, if we use two photo detectors at x_1 and x_2 to measure the joint probability $\mathcal{P}_{12}(x_1, x_2) \delta x_1 \delta x_2$, of detecting a photon within δx_1 and δx_2 , we have (Ghosh, Hong, Ou and Mandel [1986])

$$\mathcal{P}_{12}(x_1, x_2) \delta x_1 \delta x_2 = 2K_1 K_2 \delta x_1 \delta x_2 \left[1 + \cos \left(\frac{2\pi(x_1 - x_2)}{L} \right) \right], \quad (5.3)$$

where $L = \lambda/\theta$ is the spacing of the second-order interference fringes corresponding to the geometry of fig. 5.1. We can regard the effects observed as interference between two different, two-photon probability amplitudes, because the system cannot distinguish between photons from A and B being detected at x_1 and x_2 , respectively, or *vice versa*. As can be seen from eq. (5.3), the fourth-order interference fringes have a visibility of unity. On the other hand, with classical fields, it can be shown (Mandel [1983]) that the visibility of the fourth-order interference fringes cannot exceed 0.5, and the joint probability $\mathcal{P}_{12}(x_1, x_2) \delta x_1 \delta x_2$ never drops to zero.

Figure 5.2 is a schematic of the experimental arrangement used to observe the fourth-order interference fringes (Ghosh and Mandel [1987]). The beam from an argon-ion laser ($\lambda = 351.1$ nm) incident on a LiO_3 crystal generates photon pairs (see § 2.5.2) which are reflected through an interference filter so that they come together in a plane at a distance of 1.1 m at an angle of about 2° . The interference

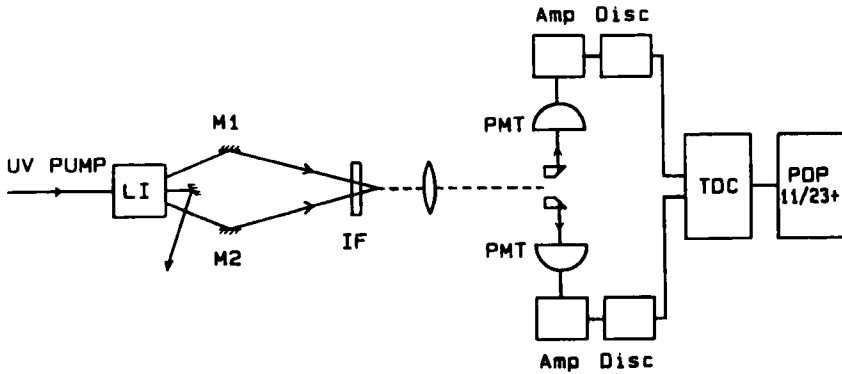


Fig. 5.2. Apparatus used to demonstrate fourth-order interference with a two-photon source (Ghosh and Mandel [1987]).

pattern formed in this plane is reimaged by a lens so as to give a spacing of the fourth-order interference fringes $L = 0.34$ mm. Two movable glass plates of thickness $\Delta x = 0.14$ mm collect the photons at x_1 and x_2 and direct them to two photomultipliers, whose outputs are fed to a counter. The number of coincidences was recorded over 10-hour periods for different values of the separation $(x_1 - x_2)$ of the plates. These values were corrected for accidental coincidences by making measurements with a delay extending from 35 to 75 ns, and subtracting the proportionate number expected within the 5 ns resolving time.

In practice, because of the finite width Δx of the detectors, the observed values of visibility are reduced by a factor:

$$\eta = \left[\frac{\sin(\pi\Delta x/L)}{\pi\Delta x/L} \right]^2. \tag{5.4}$$

Figure 5.3 shows the experimental values superimposed on a plot of the values of $\mathcal{P}_{12}(x_1, x_2)$ for a two-photon source corrected for this effect, and with the scale chosen to give the best fit with the measured coincidence rates (the solid curve). The corresponding curve from classical theory (the broken curve) is obviously a much poorer fit.

A more striking example of a nonclassical fourth-order interference effect can be observed when the inputs to the opposite sides of a beam splitter are one-photon Fock states (Fearn and Loudon [1987, 1989], Ou, Hong and Mandel [1987]). As shown in fig. 5.4, the superimposed beams leaving the beam splitter go to two photo detectors, D1 and D2, and measurements are made of the rate at which photons are detected in coincidence as the beam splitter is displaced in small steps $c\Delta\tau$ from the point where the two optical paths are equal. A sharp

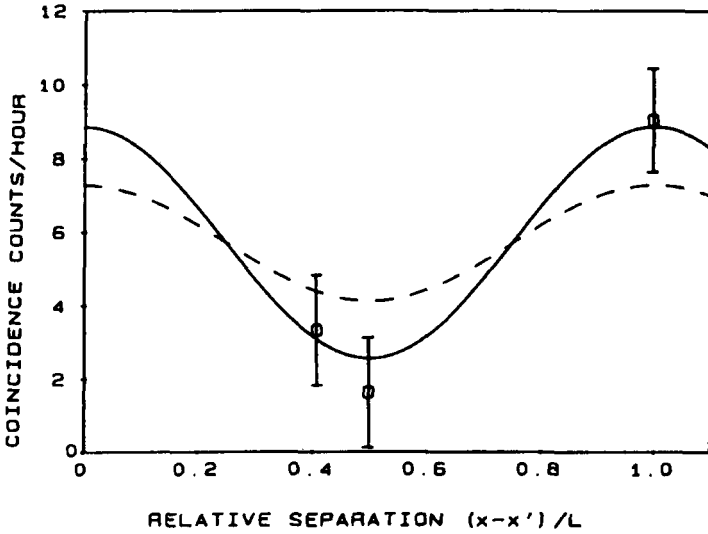


Fig. 5.3. Experimental results and predictions of quantum theory (solid curve) and classical theory (dashed curve) (Ghosh and Mandel [1987]).

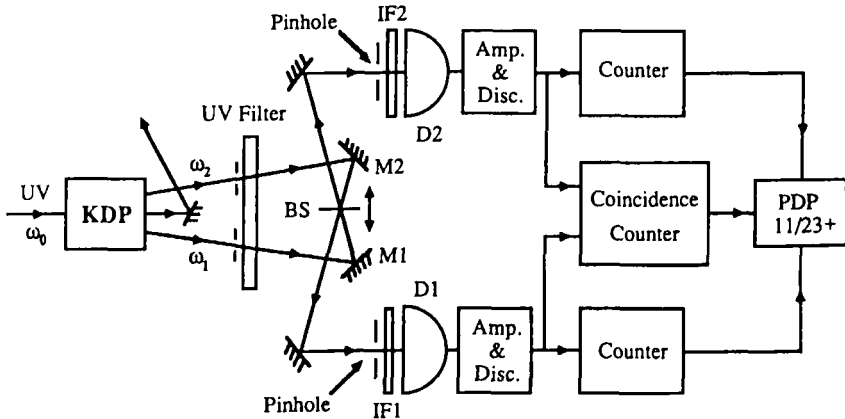


Fig. 5.4. Experimental arrangement used to demonstrate fourth-order interference effects with a varying optical path difference (Hong, Ou and Mandel [1987]).

reduction in the coincidence count rate occurs when the beam splitter occupies a symmetrical position (Hong, Ou and Mandel [1987], Rarity and Tapster [1989]).

We can label the field modes on the input sides of the beam splitter as $01, 02$ and on the output side as $1, 2$ and assume that the light is perfectly monochromatic. If the input state resulting from degenerate down-conversion

is the two-photon Fock state $|1\rangle_{01} |1\rangle_{02}$, then the state on the output side of the beam splitter is:

$$|\psi_{\text{out}}\rangle = (R - T) |1\rangle_1 |1\rangle_2 + i(2RT)^{1/2} [|2\rangle_1 |0\rangle_2 + |0\rangle_1 |2\rangle_2], \quad (5.5)$$

where R and T are the reflectance and transmittance of the beam splitter, with $R + T = 1$. It follows that for a beam splitter with $R = \frac{1}{2} = T$, the first term on the right-hand side of eq. (5.5) is zero, corresponding to destructive interference of the two-photon probability amplitudes, and the entangled state $|2; 0\rangle_{1,2}^{\pi/2, 0}$ is obtained. This state is analogous to the single-photon entangled state defined by eq. (2.14), except that in this case, it is the photon pair that is entangled with the vacuum. Alternatively, we can regard the photon pair as being in a superposition state of adopting either path 1 or path 2. No coincidences should therefore be recorded.

However, the down-converted photons are never monochromatic, and the two-photon state can be represented more correctly by the linear superposition

$$|\psi\rangle = \int d\omega f(\omega, \omega_0 - \omega) |1\rangle_\omega |1\rangle_{\omega_0 - \omega}, \quad (5.6)$$

where $f(\omega_1, \omega_2)$ is a weight function that is peaked at $\omega_1 = \frac{1}{2}\omega_0 = \omega_2$. The joint probability for the detection of photons at the detectors D1 and D2 at times t and $t + \tau$, respectively, is then:

$$\mathcal{P}_{12}(\tau) = K |G(0)|^2 \{ T^2 |G_0(\tau)|^2 + R^2 |G_0(2\Delta\tau - \tau)|^2 - RT [G_0^*(\tau) G_0(2\Delta\tau - \tau) + \text{c.c.}] \}, \quad (5.7)$$

where $G(\tau)$ is the Fourier transform of the weight function,

$$G(\tau) = \int f(\frac{1}{2}\omega_0 + \omega, \frac{1}{2}\omega_0 - \omega) \exp(-i\omega\tau) d\omega, \quad (5.8)$$

$G_0(\tau) \equiv G(\tau)/G(0)$, and K is a constant characteristic of the detectors.

While the coincidence measurement corresponds to an integration of the probability $\mathcal{P}_{12}(\tau)$ over the resolving time of a few nanoseconds, this time is so much longer than the correlation time that we may integrate $\mathcal{P}_{12}(\tau)$ over all

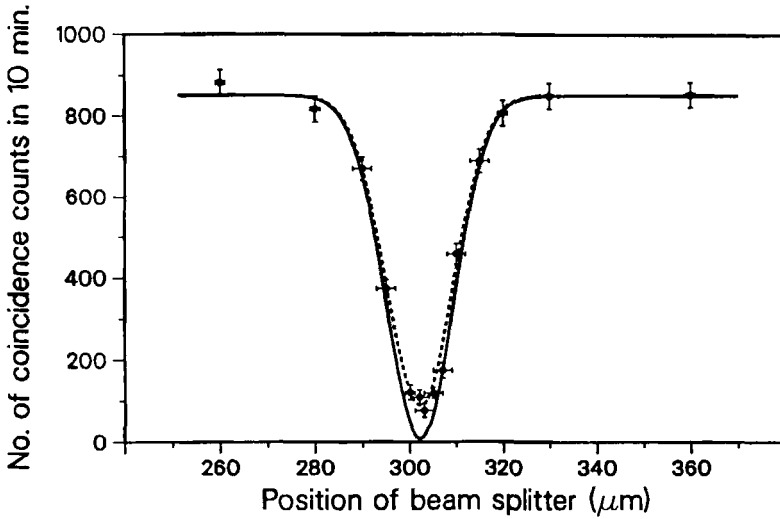


Fig. 5.5. Measured number of coincidences as a function of the displacement of the beam splitter, superimposed on the theoretical (solid) curve derived from eq. (5.10) with $R/T=0.95$ and $\Delta\omega=3\times 10^{13}$ rad/s. The dashed curve was obtained by multiplying the factor $2RT/(R^2+T^2)$ in eq. (5.10) by 0.9 (Hong, Ou and Mandel [1987]).

values of τ to obtain the expected number of observed coincidences. We then have:

$$N_c = C \left[R^2 + T^2 - 2RT \frac{\int_{-\infty}^{\infty} G_0(\tau) G_0(\tau - 2\Delta\tau) d\tau}{\int_{-\infty}^{\infty} G_0^2(\tau) d\tau} \right], \quad (5.9)$$

where C is a constant, which, when $f(\frac{1}{2}\omega_0 + \omega, \frac{1}{2}\omega_0 - \omega)$ is a Gaussian with bandwidth $\Delta\omega$, reduces to

$$N_c = C(T^2 + R^2) \left[1 - \frac{2RT}{R^2 + T^2} \exp(-\Delta\omega\delta\tau)^2 \right]. \quad (5.10)$$

It follows that when $\Delta\tau=0$, $N_c = C(R-T)^2$, which vanishes when $R = \frac{1}{2} = T$, whereas when $\Delta\tau \gg G_0(\tau)$, one has $N_c = C(T^2 + R^2)$.

Figure 5.5 shows the number of coincidences observed, after subtracting accidentals, as a function of the displacement of the beam splitter. The rate of coincidences drops to a few percent of its normal value when the two optical paths are equal, because of destructive interference of the two-photon probability amplitudes. The width of the dip in the coincidence rate yields a measure of the length of the photon wave packet which agrees with the value derived from the width of the passband of the interference filters F1 and F2.

The occurrence of an almost complete null at the center of the dip confirms that this is a nonclassical effect, since according to classical theory, the visibility cannot exceed 0.5 (Mandel [1983]). The drop in the number of coincidences is associated with an increase in the number of photon pairs leaving the beam splitter in the same direction. This behavior arises from the Bose–Einstein commutation properties of the photon-creation and annihilation operators (Fearn and Loudon [1989]).

An extension of this experiment (Ou and Mandel [1988b]) involves the use of interference filters with pass bands centered on different, nonoverlapping frequencies, ω_1 and ω_2 . If the complex frequency responses of these filters can be described by Gaussian functions with an rms width σ , the measured coincidence detection probability is:

$$\begin{aligned} \mathcal{P}_{12} \propto \sqrt{2} \pi \sigma^3 \exp \left[-\frac{(\omega_1 + \omega_2 - \omega_0)^2}{2\sigma^2} \right] \\ \times \left[T^2 + R^2 - 2TR \exp \left(\frac{-\sigma^2 \Delta \tau^2}{2} \right) \cos(\omega_1 - \omega_2) \Delta \tau \right], \end{aligned} \quad (5.11)$$

which is a maximum when the two center frequencies are chosen to satisfy the condition $\omega_1 + \omega_2 = \omega_0$. If $T = R = \frac{1}{2}$, eq. (5.11) describes an interference pattern whose visibility is unity at the center, but falls off exponentially to either side. At the center, where $\Delta \tau = 0$, the probability of coincidences $\mathcal{P}_{12} = 0$.

In the actual experiment, the pass bands of the two interference filters were centered on conjugate wavelengths of 680 and 725 nm, corresponding to a frequency difference $(\omega_1 - \omega_2)/2\pi = 27 \times 10^{12}$ Hz. Figure 5.6 shows the observed two-photon coincidence rate as a function of the position of the beam splitter and the corresponding time delay $\Delta \tau$ between the signal and idler photons. The coincidence rate exhibits interference effects with a spatial period of 5.5 μm , corresponding to a temporal period of 37 fs, which is almost exactly the period of the beat frequency. This beat frequency is observed even though neither of the photo detectors individually registers a beat.

This experiment also reveals a violation of classical theory. In addition, it demonstrates that even though there are fundamental quantum limits in attempting to localize the position of a photon to better than a few wavelengths in space, or better than a few periods in time (Newton and Wigner [1949]), this limit does not apply to the average time interval between photons, which can always be determined with subperiod precision.

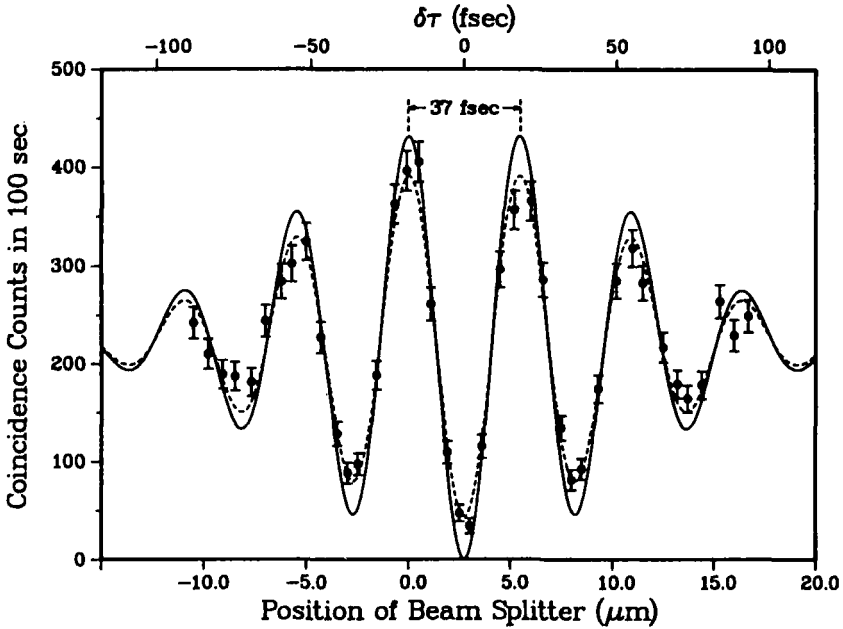


Fig. 5.6. Measured number of coincidences in 100 s as a function of the position of the beam splitter, or the time delay $\Delta\tau$, between the signal and idler photons, along with the theoretical (solid) curve obtained from eq. (5.11) and the (dotted) curve obtained when the interference term was multiplied by 0.8 (Ou and Mandel [1988b]).

5.2. INTERFERENCE IN SEPARATED INTERFEROMETERS

Fourth-order interference effects also arise when pairs of photons enter one or more interferometers, and the coincidence rate is monitored at the output ports (Kwiat, Vreka, Hong, Nathel and Chiao [1990], Ou, Zou, Wang and Mandel [1990a], Rarity, Tapster, Jakeman, Larchuk, Campos, Teich and Saleh [1990]).

In the arrangement used by Ou, Zou, Wang and Mandel [1990a] (see fig. 5.7), the two photons traveled to two photo detectors *via* two unbalanced Michelson interferometers, which were adjusted so that the difference in the propagation time between the longer and shorter paths was the same in both channels and was much greater than the coherence time of the individual photons. Under these conditions, the count rate registered by the two detectors showed no dependence on the optical path difference in either of the interferometers. However, measurements of the two-photon coincidence rate, as a function of the position of one of the mirrors, revealed interference fringes with a spatial period corresponding to the wavelength of the pump beam. A visibility of

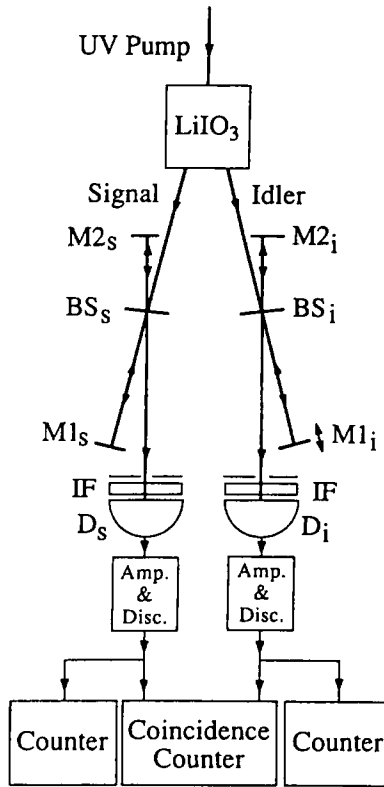


Fig. 5.7. Experimental arrangement used to observe fourth-order interference effects with photon pairs in two separated channels (Ou, Zou, Wang and Mandel [1990a]).

0.5 was obtained in this experiment, but this was due to the limited time-resolution of the detector system, and subsequent measurements with higher time-resolution gave coincidence fringes with a visibility of 0.87 (Brendel, Mohler and Martienssen [1991]).

Unusual interference patterns have also been observed with nondegenerate photon pairs (Larchuk, Campos, Rarity, Tapster, Jakeman, Saleh and Teich [1993]). In their experiments, pairs of photons whose center wavelengths differed by approximately 40 nm were used as the inputs to single and dual Mach-Zehnder interferometers (MZI). In the single MZI configuration, the paths of both down-converted beams overlapped completely within the interferometer. In the dual MZI configuration, their paths did not overlap; this is equivalent to sending each beam into a separate interferometer. Second-order interference was observed by counting the number of photons at each of the output ports, while

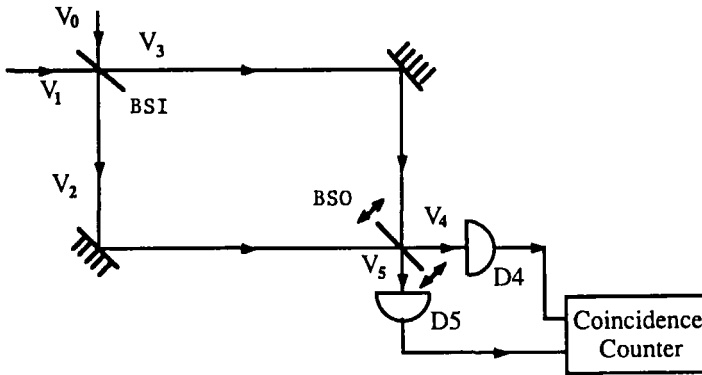


Fig. 5.8. Experimental arrangement used to study interference by two-photon superposition states formed by pairs of photons at a beam splitter (Ou, Zou, Wang and Mandel [1990b]).

observations of fourth-order interference were made by recording coincidences. Observations were made as the optical path difference was varied from zero to very large values.

The second-order interference pattern at both the output ports was the same for photon pairs as that predicted by classical theory for the center frequencies, ω_1 and ω_2 , and as expected, disappeared when the optical path difference exceeded the second-order coherence length. However, the fourth-order interference patterns were found to be quite different. For small path differences, the coincidence rates exhibited interference fringes corresponding to the difference frequency $\omega_d = |\omega_1 - \omega_2|$, as well as the sum frequency $\omega_s = |\omega_1 + \omega_2|$, when the beams overlapped, and also when they did not overlap. When the beams did not overlap, interference fringes corresponding to the center frequencies, ω_1 and ω_2 , were also observed. A striking observation was the existence of interference effects at the sum (pump) frequency at path-length differences that were greater than the second-order coherence length. This is a nonlocal quantum effect, confirming the high degree of entanglement of the down-converted photons.

In another fourth-order interference experiment (Ou, Zou, Wang and Mandel [1990b]), two photons produced simultaneously provided the two inputs to a Mach-Zehnder interferometer, as shown in fig. 5.8, and the photons emerging at the two outputs were counted. The rate of coincidences was found to exhibit interference fringes with high visibility when the optical path difference was varied, despite the fact that the two average output intensities did not vary with the optical path difference. The effects observed can be attributed to the fact that when two similar photons simultaneously enter a beam splitter at ports 0 and 1,

two photons always emerge together either at port 2 or at port 3 (Hong, Ou and Mandel [1987]), so that the output from these ports is in a superposition state. The resulting fourth-order interference fringes have a visibility of unity and are a consequence of the interference of photon pairs, rather than single photons.

5.3. THE GEOMETRIC PHASE

As described in § 4, earlier observations of the geometric (Pancharatnam) phase were made either at low light levels with classical sources, or with single-photon states. In both cases, there is no difference in the effects predicted by a classical treatment or a quantum-mechanical treatment, since the measurements only involve second-order interference.

The effects produced by the geometric (Pancharatnam) phase in fourth-order interference have been studied by Brendel, Dultz and Martienssen [1995] using the experimental arrangement shown in fig. 5.9. In this setup, photon pairs generated by down-conversion of blue light ($\lambda = 458 \text{ nm}$) from an argon-ion laser in a beta barium borate (BBO) crystal traversed a Michelson interferometer. One arm of this interferometer contained two quarter-wave plates, one of which was fixed at an azimuth of 45° , while the other could be rotated. A rotation of the second quarter-wave plate through an angle θ introduced geometric (Pancharatnam) phases $\Delta\phi = \pm 2\theta$, respectively, for the two orthogonal polarizations.

Experiments were carried out using two BBO crystals cut, respectively, for type-I and type-II phase matching, so that the photons of a pair could be prepared either in the same state of polarization (type-I) or in orthogonal states of polarization (type-II).

The photon pairs emerging from the interferometer were incident on a second beam splitter BS_2 which directed them to two photo detectors D_1 and D_2 . With type-I phase matching, BS_2 was a normal beam splitter, while with type-II phase matching, BS_2 was a polarizing beam splitter.

Measurements with this system showed that the effects observed depended on the initial states of polarization of the two photons in a pair and the optical path difference. With near-zero optical path differences, second-order interference fringes were observed, and the effects of the dynamic phase and the geometric phase were equivalent. With large optical path differences and coincidence detection, no interference was observed due to the geometric phase with type-II phase matching. However, with type-I phase matching, interference fringes with a visibility of 0.78 were obtained with a period equal to half that expected with a classical light field.

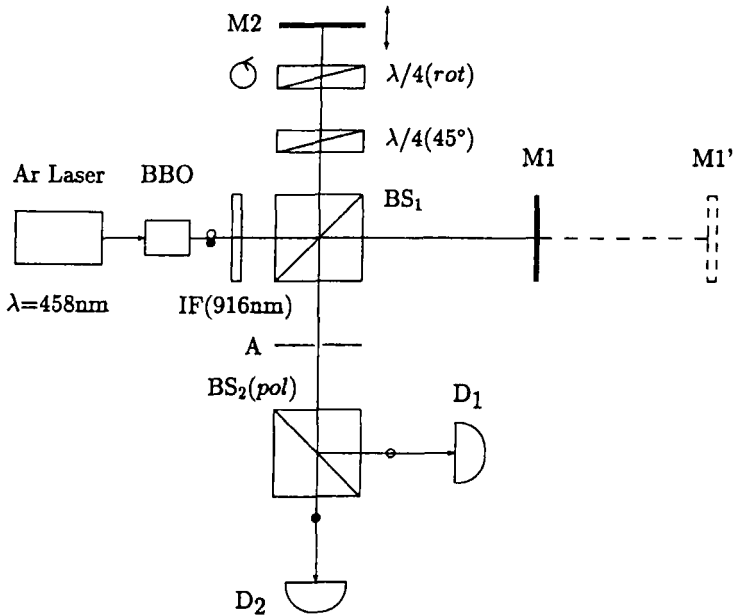


Fig. 5.9. Experimental setup used to demonstrate the effects of the geometric phase in fourth-order interference (Brendel, Dultz and Martienssen [1995]).

These results imply that pairs of photons with parallel polarizations acquire twice the geometric phase of single photons and behave like single particles with spin 2. On the other hand, pairs of photons with orthogonal polarizations acquire geometric phases with opposite signs and behave like a single particle with total spin 0. It follows that the equivalence between the dynamical phase and the geometric phase observed with second-order interference does not always exist with fourth-order interference.

5.4. TESTS OF QUANTUM THEORY

According to an alternative interpretation of quantum theory (de Broglie [1969]), the wave function describes a real physical wave, so that waves associated with different particles may interfere. An experiment to test a modified version of this theory (Croca, Garuccio, Lepore and Moreira [1990]) was performed by Wang, Zou and Mandel [1991] using the experimental arrangement shown in fig. 5.10.

If we assume 50:50 beam splitters, no idler photons will reach D_2 , but signal photons will be detected one-fourth of the time. Idler photons will only reach D_1 , and this will happen one-fourth of the time. Due to second-order interference,

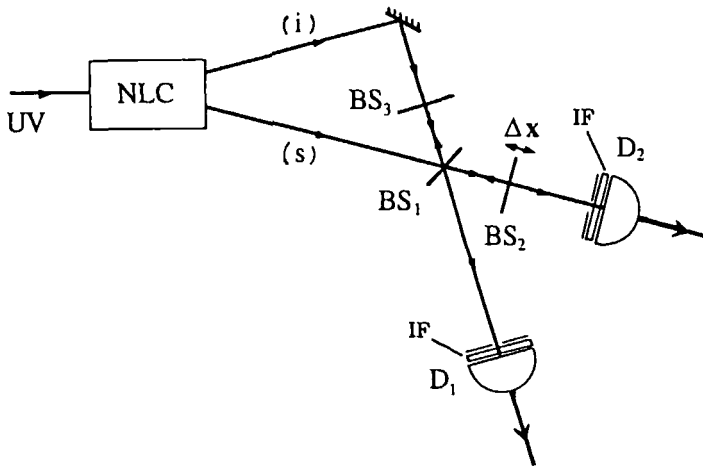


Fig. 5.10. Schematic of the experimental arrangement used to test the de Broglie guiding-wave theory (Wang, Zou and Mandel [1991]).

the rate at which signal photons reach D_1 will depend on the difference in the lengths of the optical paths from BS_1 to BS_2 and BS_3 , resulting in interference fringes with a visibility of 0.5.

However, if we consider the rate of coincidences between D_1 and D_2 , quantum theory predicts that this will be a constant, corresponding to the detection of an idler photon at D_1 and a signal photon at D_2 . On the other hand, the theory of Croca, Garuccio, Lepore and Moreira [1990] predicts coincidence fringes with a visibility of 0.5 arising from the interference of the guiding wave for the signal photon reflected from BS_3 with the guiding wave for the idler photon.

The results of this experiment revealed no such interference effects, supporting the quantum theory (however, see Holland and Vigier [1991]).

§ 6. Two-photon Interferometry

In a classic paper, Einstein, Podolsky and Rosen [1935] presented a paradox which brought out the incompatibility of quantum theory and the assumption of local realism. They were led to conclude that the quantum-mechanical description of a system was incomplete and postulated the existence of "hidden variables", the specification of which would predetermine the results of any measurements. Subsequently, Bell [1965] proposed a test, based on a *Gedankenexperiment* of Bohm [1951] involving spin-half particles, that could

distinguish between quantum theory and the entire class of theories based on local realism.

At the quantum level, polarization is associated with the spin of the photon. Although the photon is a spin-one particle, only two polarization states are allowed; hence, the angular momentum of the photon corresponds to that of a pseudo spin-half system. Polarization-correlation experiments therefore provide a convenient way to realize spin-half particle experiments. This led to a generalization of Bell's theorem, and a proposal for an experiment involving measurements of the polarization correlations of photon pairs produced by an atomic cascade (Clauser, Horne, Shimony and Holt [1969]).

6.1. ENTANGLED STATES AND BELL'S INEQUALITY

If we consider a pair of photons described by the entangled polarization singlet-like state,

$$|H; V\rangle_{1,2} = 2^{-1/2} (|H\rangle_1 |V\rangle_2 - |V\rangle_1 |H\rangle_2), \quad (6.1)$$

where H and V denote single photons with horizontal and vertical polarizations, respectively, and the subscripts identify their propagation directions, a measurement involving photons travelling in one of these directions will show no preferred polarization. However, if the polarization of photon 1 is measured in some basis, the polarization of photon 2 can be predicted with certainty. We then find that while quantum mechanics and theories based on local realism agree in situations of perfect correlations or anticorrelations, quantum mechanics gives different predictions for polarizers at intermediate angles (Clauser, Horne, Shimony and Holt [1969]).

Initially, experimental tests of Bell's inequality, based on polarization correlations, were made using pairs of photons produced by an atomic cascade (Aspect, Dalibard and Roger [1982]). However, in these experiments the correlation of the polarizations was not complete because of the imperfect angular correlation of the photons.

Better results have been obtained in experiments using pairs of photons produced by parametric down-conversion (Shih and Alley [1988], Ou and Mandel [1988a]). In the arrangement used by Ou and Mandel [1988a] (see fig. 6.1), linearly polarized photons (wavelength about 702 nm) with their electric vector in the plane of the diagram were produced by degenerate parametric down-conversion. The idler photons passed through a half-wave plate that rotated their plane of polarization by 90° , while the signal photons traversed a compensating

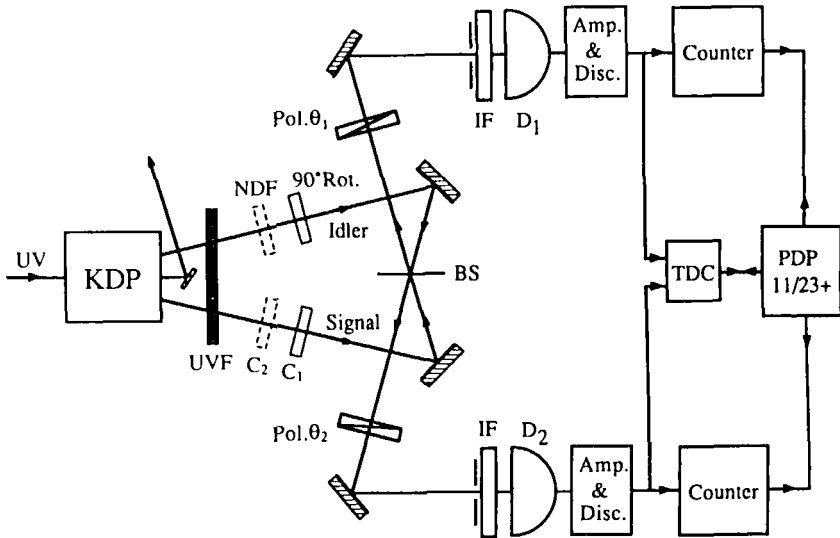


Fig. 6.1. Apparatus used to demonstrate violations of Bell's inequality using photon pairs produced by parametric down-conversion (Ou and Mandel [1988a]).

glass plate producing an equal time delay. The mixed signal and idler photons emerging from the two sides of the beam splitter, after passing through linear polarizers set at adjustable angles θ_1 and θ_2 and identical interference filters, were incident on two photodetectors D_1 and D_2 . The coincidence counting rate provided a measure of the joint probability $\mathcal{P}(\theta_1, \theta_2)$ of detecting two photons for various settings θ_1, θ_2 of the two linear polarizers.

According to quantum theory, the probability of detecting a coincidence in this arrangement is:

$$\mathcal{P}(\theta_1, \theta_2) \propto \sin^2(\theta_2 - \theta_1), \quad (6.2)$$

which only depends on the difference in the angular settings of the two polarizers. The actual coincidence count rates obtained for various values of θ_1 , with θ_2 fixed at 45° , are presented in fig. 6.2, along with curves corresponding to the predictions of quantum mechanics and classical theory. As can be seen, the observed relative modulation obtained from the best fit curve is about 0.76, which is below the value of 1.00 predicted by quantum mechanics, probably because of imperfect alignment of the signal and idler beams, but greater than the figure of 0.50 expected from classical theory. However, this result corresponds to a violation of Bell's inequality by about 6 standard deviations.

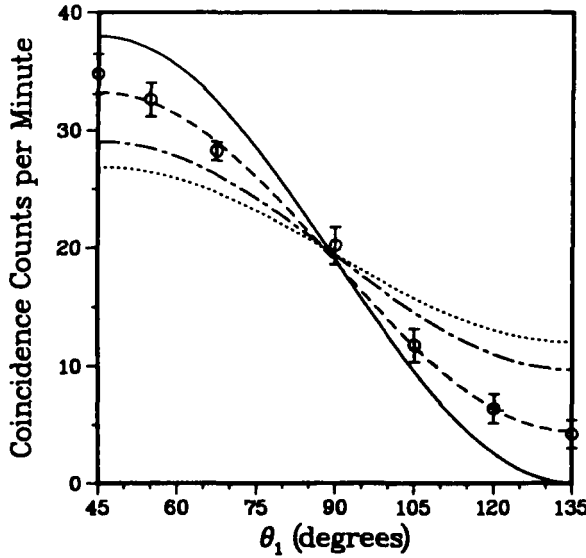


Fig. 6.2. Measured coincidence counting rate for different values of the polarizer angle θ_1 , with θ_2 fixed at 45° . The solid curve and the dash-dotted curve correspond to the predictions of quantum mechanics and classical theory, respectively. The dashed and dotted curves are obtained by multiplying these curves by a factor of 0.76 to allow for reduced modulation due to imperfect alignment of the beams (Ou and Mandel [1988a]).

6.2. INTERFEROMETRIC TESTS OF BELL'S INEQUALITY

The generation of correlated photon pairs by parametric down-conversion has also made possible tests of Bell's inequality using two-photon interferometry, which are not based on polarization (Horne, Shimony and Zeilinger [1989]).

A general arrangement for two-photon interferometry is shown in fig. 6.3. In this arrangement, pairs of photons, one having a wavelength λ_1 and the other a wavelength λ_2 , are selected by four pinholes in a diaphragm placed downstream from the nonlinear crystal to produce four beams, A, B, C, D , with wave vectors k_A, k_B, k_C and k_D , where

$$|k_A| = |k_D|, \quad (6.3)$$

$$|k_B| = |k_C|, \quad \text{but} \quad |k_B| \neq |k_A|, \quad (6.4)$$

and

$$k_A + k_C = k_B + k_D = k, \quad (6.5)$$

where k is the wave vector of the beam incident on the crystal.

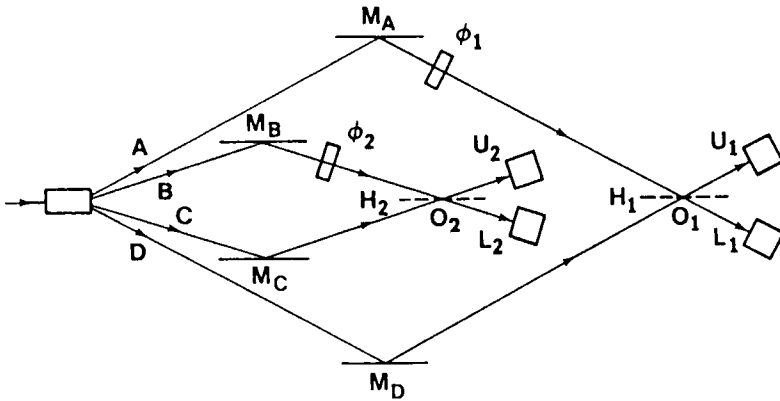


Fig. 6.3. Schematic of an interferometer used to demonstrate two-photon interference (Horne, Shimony and Zeilinger [1989]).

Each pair in the ensemble of photon pairs is in the quantum state

$$|\psi\rangle = 2^{1/2} [|A\rangle_1 |C\rangle_2 + |D\rangle_1 |B\rangle_2], \tag{6.6}$$

which is a coherent superposition of the probability amplitudes corresponding to two distinct pairs of correlated paths. In one case, a photon with wavelength λ_1 goes into beam *A*, and a photon with wavelength λ_2 goes into beam *C*; in the other, a photon with wavelength λ_1 goes into beam *D*, and a photon with wavelength λ_2 goes into beam *B*. A variable phase difference ϕ_1 can be introduced between the beams *A* and *D* before they are recombined by the 50:50 beam splitter H_1 and proceed to the photo detectors U_1 and L_1 . Similarly, a variable phase difference ϕ_2 can be introduced between the beams *B* and *C* before they are recombined by the 50:50 beam splitter H_2 and proceed to the photo detectors U_2 and L_2 . It follows that the two interfering beams at H_1 have the same wavelength λ_1 , while the two interfering beams at H_2 have the same wavelength λ_2 ; however, the wavelengths at H_1 and H_2 are different.

The quantum-mechanical probabilities for the joint detection of both photons by the detector pairs (U_1, U_2) , (L_1, L_2) , (U_1, L_2) , and (U_2, L_1) , are then proportional to the absolute squares of the corresponding probability amplitudes defined by eq. (6.6), and are given by the relations:

$$\begin{aligned} \mathcal{P}(U_1, U_2 | \phi_1, \phi_2) &= \mathcal{P}(L_1, L_2 | \phi_1, \phi_2) \\ &= \frac{1}{4} \eta^2 [1 + \cos(\phi_2 - \phi_1 + \phi_0)], \end{aligned} \tag{6.7}$$

and

$$\begin{aligned} \mathcal{P}(U_1, L_2 | \phi_1, \phi_2) &= \mathcal{P}(L_1, U_2 | \phi_1, \phi_2) \\ &= \frac{1}{4} \eta^2 [1 - \cos(\phi_2 - \phi_1 + \phi_0)], \end{aligned} \tag{6.8}$$

where η is the quantum efficiency of the photo detectors, and ϕ_0 is a phase factor determined, once and for all, by the placement of the mirrors and beam splitters.

On the other hand, the probabilities for detecting single photons by the four detectors are:

$$\begin{aligned} \mathcal{P}(U_1 | \phi_1, \phi_2) &= \mathcal{P}(L_1 | \phi_1, \phi_2) = \mathcal{P}(U_2 | \phi_1, \phi_2) = \mathcal{P}(L_2 | \phi_1, \phi_2) \\ &= \frac{1}{2} \eta. \end{aligned} \quad (6.9)$$

It follows that while the count rate for single photons, which is defined by eq. (6.9), is constant and independent of ϕ_1 and ϕ_2 , the count rates for coincidences, which are defined by eqs. (6.7–6.8), will vary sinusoidally with the phase shifts ϕ_1 and ϕ_2 . These interference fringes observed with spatially separated two-photon states are a quantum-mechanical phenomenon arising from their entangled nature.

An experimental arrangement involving two-photon interferometry, similar to that shown in fig. 6.3, was used by Rarity and Tapster [1990] for a test of Bell's inequality based on the entanglement of the momenta of the photons in a pair. In this case, given the direction of one photon at one of the detectors U_2, L_2 , quantum theory indicates that the direction taken by the other photon of the pair is dependent on the setting of the remote phase plate ϕ_2 to an extent that cannot be explained by any theory based on local realism.

To verify this proposition, measurements were made of the coincidence rates between the four detectors for selected values of the variable phase differences. The correlation coefficient

$$\mathcal{E}(\phi_1, \phi_2) = \frac{\mathcal{P}(U_1, U_2 | \phi_1, \phi_2) + \mathcal{P}(L_1, L_2 | \phi_1, \phi_2) - \mathcal{P}(U_1, L_2 | \phi_1, \phi_2) - \mathcal{P}(L_1, U_2 | \phi_1, \phi_2)}{\mathcal{P}(U_1, U_2 | \phi_1, \phi_2) + \mathcal{P}(L_1, L_2 | \phi_1, \phi_2) + \mathcal{P}(U_1, L_2 | \phi_1, \phi_2) + \mathcal{P}(L_1, U_2 | \phi_1, \phi_2)}, \quad (6.10)$$

can be taken as a measure of the distribution of coincidences between detectors on the same side and opposite sides of the beam splitters for these phase settings.

A generalization of Bell's inequality (Clauser and Shimony [1978]) then states that the combination of four such measurements, at various phase settings given by the relation

$$S = \mathcal{E}(\phi_1, \phi_2) - \mathcal{E}(\phi_1, \phi'_2) + \mathcal{E}(\phi'_1, \phi_2) + \mathcal{E}(\phi'_1, \phi'_2), \quad (6.11)$$

should always lie within the bounds

$$-2 \leq S \leq 2, \quad (6.12)$$

if we assume local realism. However, quantum theory indicates that for appropriately chosen values of the phase angles ($\phi_1 = 0$, $\phi'_1 = \frac{1}{2}\pi$, $\phi_2 = \frac{1}{4}\pi$, $\phi'_2 = \frac{3}{4}\pi$),

$$S = 2\sqrt{2}. \quad (6.13)$$

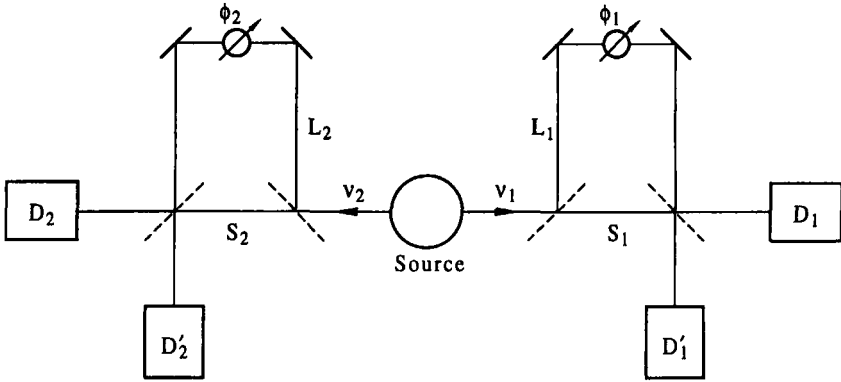


Fig. 6.4. Simplified schematic of the optical system for a Bell's inequality experiment based on energy and time correlations (Franson [1989]).

In actual measurements, a value of $S = 2.21 \pm 0.022$ was obtained. This lower value could be attributed to a reduced visibility $\mathcal{V} = 0.78$ of the interference fringes due to misalignment of the apparatus, but corresponded to a violation of Bell's inequality by 10 standard deviations.

Another experimental test of Bell's inequality was proposed by Franson [1989] and carried out by several groups (Franson [1991a], Brendel, Mohler and Martienssen [1992], Kwiat, Steinberg and Chiao [1993], Shih, Sergienko and Rubin [1993]). Figure 6.4 is a schematic of the basic arrangement. In the actual experiments, each of the photons from a down-converted pair was sent into an unbalanced interferometer, presenting a short (S) and a long (L) path to the final output.

Examination of the singles count rates when the imbalances were greater than the coherence length of the down-converted photons revealed no interference effects. However, when the difference of the path-length differences in the two interferometers was less than the coherence length of the down-converted photons, observations of the coincidence rates revealed interference effects arising from the impossibility of distinguishing between the two processes which led to coincidences. These interference effects could be observed even when the extra optical path traversed by one of the photons was quite long (Franson [1991b], Rarity and Tapster [1992]).

With detectors fast enough to exclude the possibility of one photon taking the short path, and the other taking the long path, high-visibility fringes could be obtained corresponding to observations of the quantum state

$$|\psi\rangle = \frac{1}{2} (|S_1, S_2\rangle - e^{i\phi} |L_1, L_2\rangle), \quad (6.14)$$

where ϕ is proportional to the sum of the relative phases in the two interferometers. As shown in fig. 6.5, sinusoidal fringes with a visibility greater than 0.8 were obtained (Kwiat, Steinberg and Chiao [1993]), whereas the maximum possible without violating Bell's inequality would be 0.71.

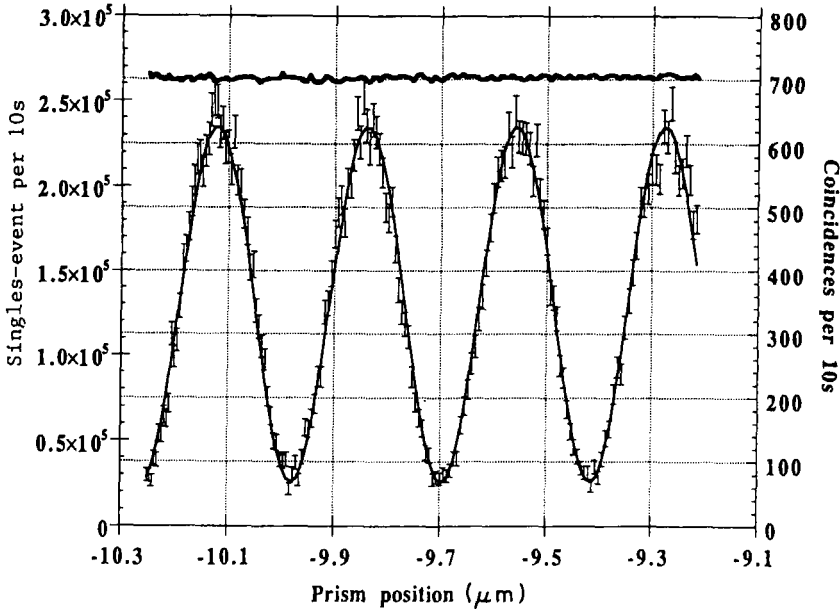


Fig. 6.5. Coincidence fringes obtained as the phase in interferometer 1 is varied. The constant single-event rate is also shown for comparison (Kwiat, Steinberg and Chiao [1993]).

A significant loophole in all these experiments has been the lack of detectors with unit quantum efficiency, necessitating the assumption that the fraction of the pairs detected is representative of the entire ensemble (Clauser, Horne, Shimony and Holt [1969], Santos [1992]). Some progress towards solving this problem has been made by the development of photo detectors with high quantum efficiencies (Kwiat, Steinberg, Chiao, Eberhard and Petroff [1993]). A possibility is the use of a nonmaximally entangled state (in which the magnitudes of the probability amplitudes of the contributing terms are not equal), which can lead to a significant reduction in the required detector efficiency (Eberhard [1993]). An experiment leading to a loophole-free test of Bell's inequality has been proposed by Kwiat, Eberhard, Steinberg and Chiao [1994].

6.3. OTHER TESTS OF LOCAL REALISM

Another solution of the problem of demonstrating that quantum mechanics violates local realism, which does not involve Bell's inequality, has been developed by Hardy [1992a,b, 1993] and by Jordan [1994]. Figure 6.6 shows the setup used by Torgerson, Branning, Monken and Mandel [1995] in an experiment based on this approach.

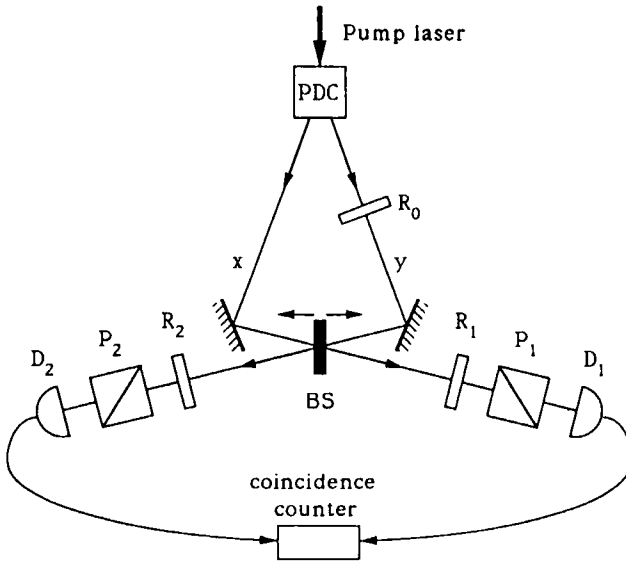


Fig. 6.6. Setup used to demonstrate violation of local realism (Torgerson, Branning, Monken and Mandel [1995]).

In this arrangement, pairs of photons with linear (x) polarizations were produced by parametric down conversion. A rotator R_0 inserted in the idler beam converted it to the orthogonal (y) polarization. The signal and idler beams were then mixed at a beam splitter, and the two outputs were taken to similar analyzers. Each of these consisted of a rotatable half-wave plate (R_1 or R_2) followed by a fixed linear polarizer (P_1 or P_2) and a photo detector (D_1 or D_2).

We consider measurements of the number of two-photon coincidences made with a series of polarizer settings when the signal and idler optical path lengths are equal. The angles θ_1 and θ_{10} define two possible settings of the polarizer in arm 1; similarly, θ_2 and θ_{20} define two possible settings of the polarizer in arm 2. The angles $\bar{\theta}_i = \theta_i + \frac{1}{2}\pi$ ($i=1, 2, 10, 20$) define the orthogonal settings. If $\mathcal{P}_{12}(\theta_1, \theta_2)$ is the joint probability of detecting a photon in arm 1 with the

polarizer set at θ_1 and a photon in arm 2 with the polarizer set at θ_2 , quantum mechanics shows that, for a nonabsorbing beam splitter with $|T|^2 + |R|^2 = 1$ and $|T| \neq |R|$, there exist polarizer angles θ_1 , θ_2 , θ_{10} , $\bar{\theta}_{10}$, θ_{20} and $\bar{\theta}_{20}$, such that

$$\mathcal{P}_{12}(\theta_1, \bar{\theta}_{20}) = 0, \quad (6.15)$$

$$\mathcal{P}_{12}(\bar{\theta}_{10}, \theta_2) = 0, \quad (6.16)$$

$$\mathcal{P}_{12}(\theta_{10}, \theta_{20}) = 0, \quad (6.17)$$

$$\mathcal{P}_{12}(\theta_1, \theta_2) > 0. \quad (6.18)$$

The value of $\mathcal{P}_{12}(\theta_1, \theta_2)$ is greatest when (Torgerson, Branning and Mandel [1995]):

$$\tan \theta_1 = \left(\frac{|T|}{|R|} \right)^3 = \cot \theta_2, \quad \tan \theta_{10} = -\frac{|T|}{|R|} = \cot \theta_{20}. \quad (6.19)$$

However, according to the point of view adopted by Einstein, Podolsky and Rosen [1935], eq. (6.18) contradicts eq. (6.17).

Experimental measurements confirmed that the value of $\mathcal{P}_{12}(\theta_1, \theta_2)$ was clearly non zero. Even though the values for $\mathcal{P}_{12}(\theta_1, \bar{\theta}_{20})$, $\mathcal{P}_{12}(\bar{\theta}_{10}, \theta_2)$ and $\mathcal{P}_{12}(\theta_{10}, \theta_{20})$ were not exactly equal to zero, the data contradicted local realism by about 45 standard deviations.

6.4. TWO-PHOTON INTERFERENCE

Another class of two-photon interference experiments makes use of the down-converted light beams from two nonlinear crystals which are optically pumped by mutually coherent beams from the same laser.

In one arrangement (see fig. 6.7), the signal beams s_1 and s_2 from the two down-converters are combined by one beam splitter (BS_A) and allowed to fall

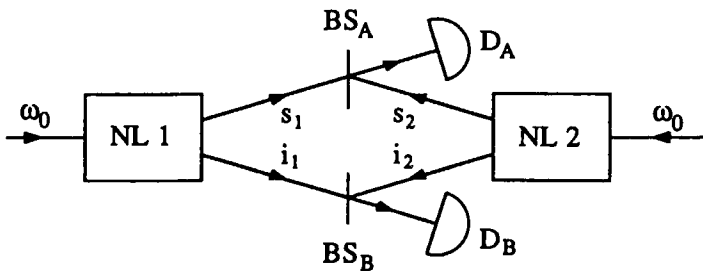


Fig. 6.7. Experimental arrangement used to observe interference effects produced by down-converted light beams from two nonlinear crystals (Ou, Wang, Zou and Mandel [1990]).

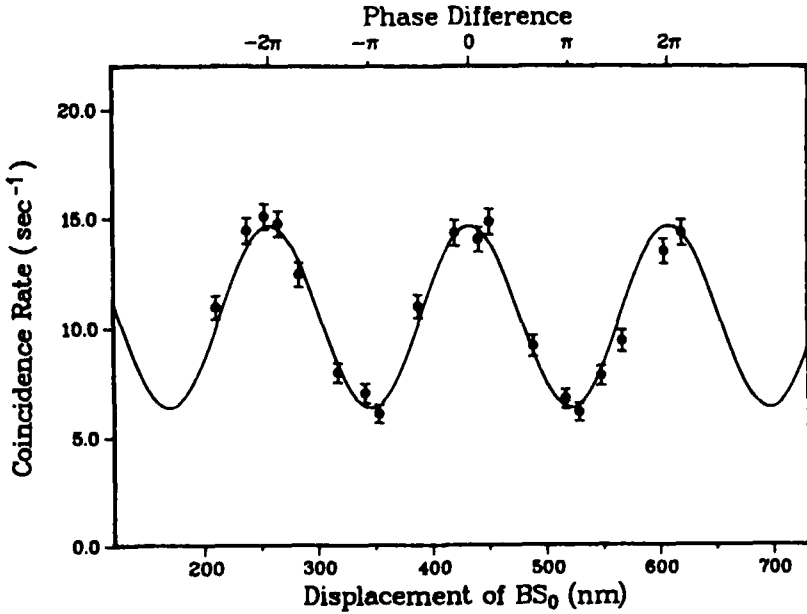


Fig. 6.8. Measured two-photon coincidence rate as a function of the displacement of the beam splitter (Ou, Wang, Zou and Mandel [1990]).

on one photo detector (D_A), while the two idler beams i_1 and i_2 are combined by another beam splitter (BS_B) and taken to another photo detector (D_B) (Ou, Wang, Zou and Mandel [1990]). Measurements of the counting rates of the individual photo detectors showed no change as the optical path difference was varied, confirming that the mutual coherence of the pump beams did not produce any mutual coherence, either between the two signal beams s_1 and s_2 from the two down-converters, or between the two idler beams i_1 and i_2 . However, as shown in fig. 6.8, measurements of the coincidence rate for simultaneous detection of photons by both D_A and D_B , as a function of the optical path difference, revealed interference effects.

A modification of this arrangement, shown in fig. 6.9, uses a single nonlinear crystal traversed by the pump beam in opposite directions (Herzog, Rarity, Weinfurter and Zeilinger [1994]). Down-converted photons can be generated on either of the two passes, and it is possible to make the idler modes from the two processes overlap at one photo detector, while the signal modes overlap at the other. Since the two production processes are indistinguishable, interference effects are observed in the singles rates, as well as in the coincidence rates, when any one of the mirrors is translated. An interesting aspect of this experiment is

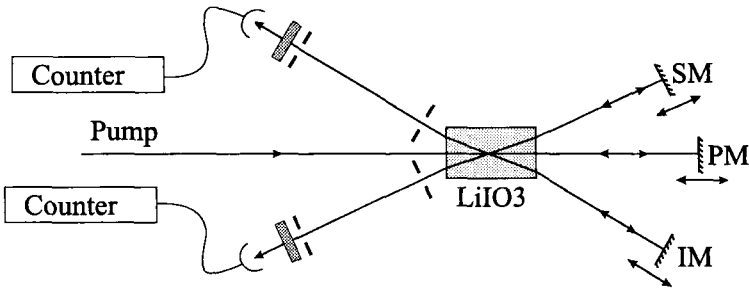


Fig. 6.9. Arrangement using a single nonlinear crystal to generate two sets of down-converted light beams (Herzog, Rarity, Weinfurter and Zeilinger [1994]).

that the distances to the mirrors can be much greater than the coherence lengths of the down-converted beams; one interpretation of the results is, therefore, a variable enhancement (or suppression) of the down-conversion process.

Nonclassical effects can also show up in certain second-order interference experiments in which only one photon is detected (Mandel [1982]). Figure 6.10 is a schematic of the optical system for such an interference experiment with beams from two parametric down-converters (Zou, Wang and Mandel [1991]). In this arrangement, both the nonlinear crystals, NL_1 and NL_2 , were optically pumped by mutually coherent beams derived from the same laser by means of a beam splitter. However, while the two signal beams s_1 and s_2 were combined by means of another beam splitter and taken to a photo detector (D_s), the idler beam i_1 was allowed to pass through the nonlinear crystal NL_2 and fall, along with the second idler beam i_2 , directly on the other photo detector D_i .

When the optical path difference was varied by translating the beam splitter BS_0 , the photon counting rate at D_s was found to oscillate, indicating that s_1 and s_2 were mutually coherent (see curve A in fig. 6.11). These oscillations could be observed as long as i_1 and i_2 were collinear, but if either i_1 or i_2 was misaligned, or if i_1 was blocked so that it could not reach NL_2 , the interference disappeared (see curve B in fig. 6.11).

If, instead of blocking i_1 , an attenuator or beam splitter with a complex amplitude transmittance t was placed between NL_1 and NL_2 , the visibility of the interference pattern registered by D_s was found to be proportional to $|t|$. However, the average rate of photon counts was the same in both cases, implying that the degree of mutual coherence of the two beams could be controlled without affecting their intensities.

In addition, the introduction of a delay τ , by varying the length of the path of the idler i_1 between the two nonlinear crystals NL_1 and NL_2 , was found to

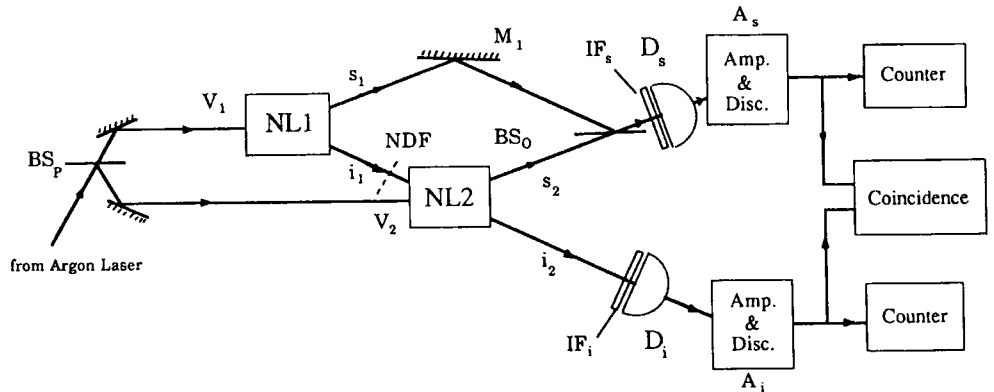


Fig. 6.10. Experimental setup used to observe interference effects produced by the signal beams from two parametric down-converters (Zou, Wang and Mandel [1991]).

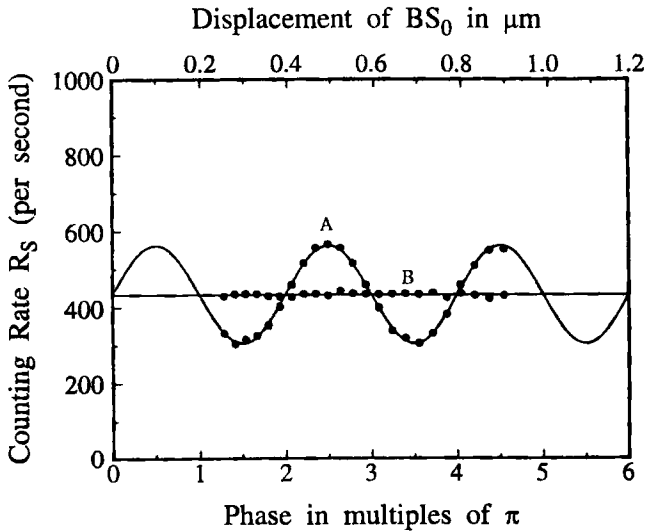


Fig. 6.11. Counting rate of the detector D_s as a function of the displacement of the beam splitter BS_0 : (A) with the idler beams i_1 and i_2 aligned and (B) with the idler beam i_1 blocked (Zou, Wang and Mandel [1991]).

affect the visibility of the interference effects produced by the signal beams, s_1 and s_2 , exactly as if the delay had been introduced in one of the signal paths (Zou, Grayson, Barbosa and Mandel [1993]). A phase shift of the idler beam i_1 introduced through the geometric (Pancharatnam) phase (see § 4.1) also had the same effect on the interference pattern produced by the signal beams (Grayson, Torgerson and Barbosa [1994]).

Figure 6.12 shows the variation of the visibility of the interference effects as a function of the time delay; as can be seen, when $\tau > \tau_c$, where $\tau_c \approx 1$ ps is the coherence time, the visibility of the interference effects drops to zero. However, it is well known that even when $\tau \gg \tau_c$, interference effects can still be seen in the spectral domain (Mandel [1962]). Such effects were observed in this experiment by inserting a scanning Fabry–Perot interferometer before the detector D_s (Zou, Grayson and Mandel [1992]). As shown in fig. 6.13, the expected modulation of the spectrum could be observed even with a differential delay $\tau \approx 5$ ps $\approx 5\tau_c$. This modulation disappeared when the idler beam i_1 was blocked.

All these effects can be understood in terms of the indistinguishability of the paths taken by the beams through the interferometer. In the arrangement shown in fig. 6.7, when a coincidence is registered, there is no way to determine whether the pair of photons involved originated in NL_1 or NL_2 . Similarly, in the

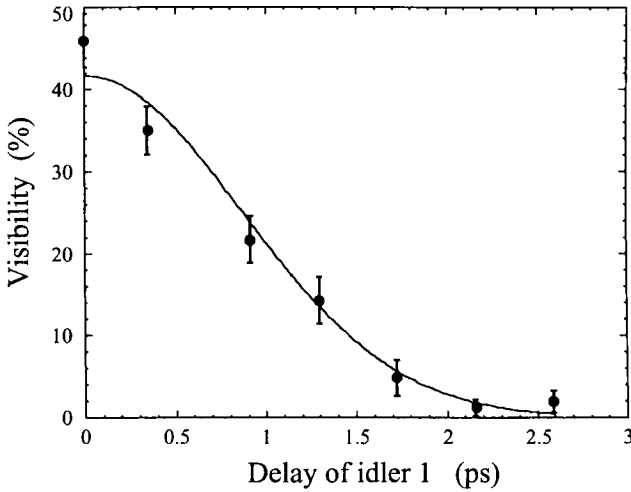


Fig. 6.12. Variation of the visibility of the interference effects produced by the signal beams s_1 and s_2 with the time delay inserted in the idler beam i_1 (Zou, Grayson, Barbosa and Mandel [1993]).

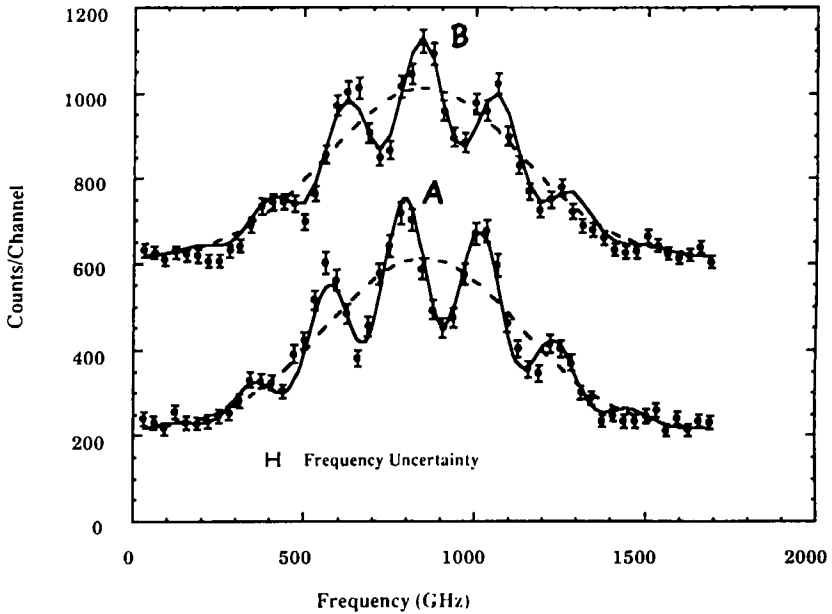


Fig. 6.13. Variation of the count rate as a function of the optical frequency with a time delay $\tau \approx 3\tau_c$ inserted in (A) s_1 and (B) i_1 . The dashed curve shows the original unmodulated spectrum (Zou, Grayson and Mandel [1992]).

arrangement shown in fig. 6.10, there is no way to determine the origins of the photons reaching the photo detector D_s , as long as both i_1 and i_2 are incident on the detector D_i .

6.5. TWO-PHOTON TESTS OF BELL'S INEQUALITY

An experimental arrangement that could overcome the problems encountered with earlier interferometric tests of Bell's inequality has been proposed by Pavičić [1995]. This arrangement is based on fourth-order spin-correlated interferometry using two independent pairs of spin-correlated photons.

Ou, Hong and Mandel [1987] showed that a pair of orthogonally polarized photons incident on a symmetrically positioned beam splitter produce a singlet-like state. On the other hand, similar photons with parallel polarizations never appear on opposite sides of the beam splitter (Hong, Ou and Mandel [1987]). Subsequently, these observations were extended to show that the fourth-order interference interaction between a beam splitter and two incoming unpolarized photons imposes polarization correlations on the emerging photons. For an appropriate position of the beam splitter, incoming unpolarized photons emerge with orthogonal polarizations. More specifically, they appear entangled in a singlet state, similar to that described by eq. (6.1), when they exit on different sides of the beam splitter (Pavičić [1994], Pavičić and Summhammer [1994]).

In the arrangement shown in fig. 6.14 (Pavičić [1995]), a subpicosecond laser pulse pumps two nonlinear crystals, NL1 and NL2, to produce simultaneous pairs of signal and idler photons with the same frequency, which are converted to orthogonal polarizations by the 90° rotators. These photon pairs are incident on the two beam splitters, BS1 and BS2, which therefore act as sources of independent singlet pairs. Two of the photons, one from each pair, interfere at the beam splitter BS. As a result, the other two photons from these pairs appear to be in a singlet state, although they are completely independent and have never interacted. Even when no polarization measurements are carried out on the first two photons, one finds polarization correlations between the latter two photons. One of the subsets of these two photons contains only photons in the singlet state, and we can therefore consider them preselected by their pair-companions which interfered at BS.

It can then be shown that, with the polarizers P1 and P2 removed, and the polarizers P1' and P2' oriented at angles $\theta_{1'}$ and $\theta_{2'}$, respectively, the probability of coincident detection of four photons by the detectors D1, D2, D1' and D2' is given by the relation

$$\mathcal{P}(\theta_{1'}, \theta_{2'}) = \frac{1}{8} [1 - \nu \cos^2(\theta_{1'} - \theta_{2'})], \quad (6.20)$$

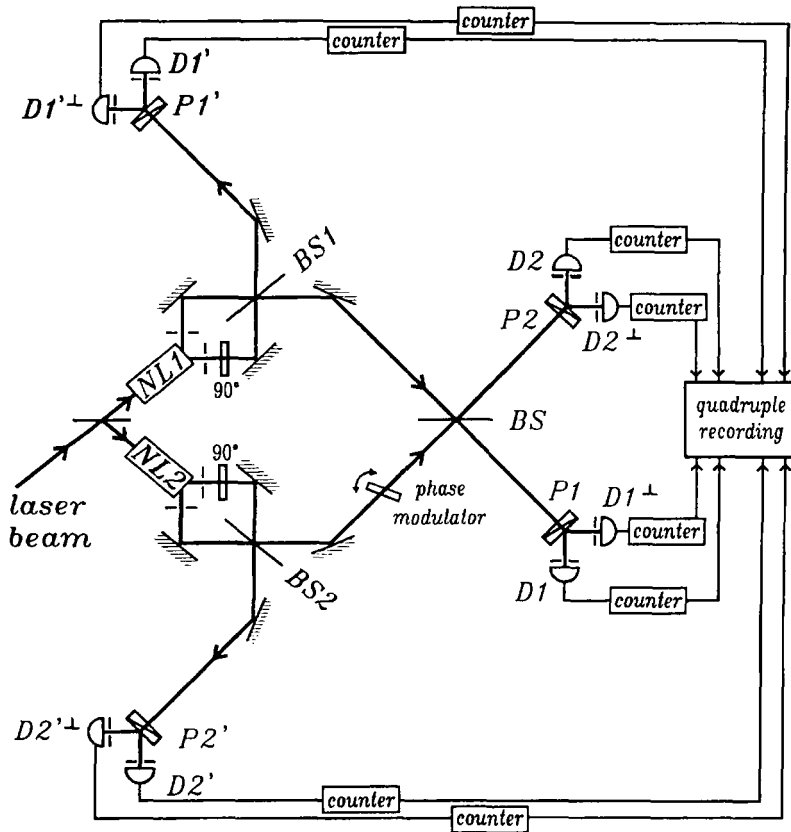


Fig. 6.14. Experimental arrangement for an interferometric test of Bell's inequality using spin-correlated photons (Pavičić [1995]).

where \mathcal{V} is the visibility of the fringes normally obtained by coincidence counting. This probability is given by the ratio of the numbers of coincidence counts,

$$f(\theta_{1'}, \theta_{2'}) = \frac{N(D1' \cap D2')}{N[(D1' \cup D1'^{\perp}) \cap (D2' \cup D2'^{\perp})]}, \tag{6.21}$$

divided by 4. For a violation of Bell's inequality, we need

$$\eta(1 + \mathcal{V}\sqrt{2}) > 2, \tag{6.22}$$

where η is the quantum efficiency of the detectors.

Pavičić [1995] has also proposed a modification that would, in principle, make it possible to lower the required threshold levels for the visibility of the interference fringes and the quantum efficiency of the detectors.

§ 7. Complementarity

Interferometry in the quantum domain is characterized by complementarity: wave *vs* particle, certainty in photon number *vs* certainty of phase, visibility of interference fringes *vs* certainty of the photon path. The paradox of the undular and corpuscular aspects of light, which flow from the quantum description, has led to many experiments to study complementarity.

In § 3.2, we discussed some experiments on interferometry with single-photon input states by Grangier, Roger and Aspect [1986]. Although the quality of the interference fringes produced by single-photon states is impressive, the most striking aspect of the experiment is the fact that the apparatus could be transformed easily to exhibit either wave-like or particle-like behavior by a single photon. At the same time, it does not follow that two distinct experiments are required to reveal complementary features of the photon. Wootters and Zurek [1979] employed an information-theoretic approach to show how, in a double-slit experiment, one could obtain some information on the path taken by the photon (particle-like behavior) while retaining an interference pattern with some degree of clarity (wave-like behavior). Measurements are not restricted therefore to either one or the other of these complementary quantities, and some information on both can always be obtained, subject to the limits set by complementarity.

7.1. QUANTUM-NONDEMOLITION MEASUREMENTS

Heisenberg's principle states that the uncertainty in the number of quanta n in a beam of light and the uncertainty in its phase ϕ are linked through the relation (Heitler [1954])

$$\Delta n \Delta \phi \geq \frac{1}{2}. \quad (7.1)$$

It follows from this relation that, if we know the exact number of photons in a beam, we have no knowledge of the phase.

However, in principle, experiments based on photon-number quantum non-demolition measurements are possible (Milburn and Walls [1983], Yamamoto, Imoto and Machida [1986], Braginsky [1989]), in which the photon number of

the light field can be measured in such a way that, following the measurement, the number of light quanta remains unchanged. Several schemes have been proposed for this purpose (Roch, Roger, Grangier, Courty and Reynaud [1992]).

One method is based on the phase shift of an electron wave produced by a light beam through the Aharonov–Bohm effect (Chiao [1970], Lee, Yin, Gustafson and Chiao [1992]). Another uses the phase shift in a probe beam resulting from the index change produced through the Kerr effect by a signal beam (Imoto, Haus and Yamamoto [1985], Kitagawa and Yamamoto [1986]). Yet other proposals use Rydberg atoms to give indirect information on the number of photons in a microwave cavity (Haroche, Brune and Raimond [1992], Walther [1992]).

Since a quantum-nondemolition measurement allows the determination of the presence of a single photon without annihilating it, complementarity requires a disturbance to the interference fringes. A theoretical treatment, by Sanders and Milburn [1989], of a photon-number quantum-nondemolition measurement in one arm of a Mach–Zehnder interferometer, with single-photon inputs into one port of the interferometer, demonstrates that the interference fringes are progressively reduced in visibility as greater certainty of the path of the photon through the interferometer is obtained. The presence of the photon is detected by the phase shift of a probe field that interacts with the photon *via* a nonlinear Kerr medium. Greater certainty of the path of the photon requires a reduction of the phase fluctuations in the probe field. This reduction requires a corresponding increase in the amplitude fluctuations of the probe field which feed, in turn, into the phase fluctuations of the field within the interferometer and destroy the interference fringes.

7.2. DELAYED-CHOICE EXPERIMENTS

An interesting question raised by von Weiszäcker [1931] and by Wheeler [1978] is whether the result of Young's double-slit experiment would be changed if the decision to observe either interference, or the path of the photon, was made after the photon had passed through the slits.

Wheeler's proposal envisaged a Mach–Zehnder interferometer illuminated by a light pulse with photo detectors placed in the two outputs. A decision would be made "whether to put in the second beam splitter, or take it out, at the very last minute". This would make it possible to decide whether the photon had come by one route, or by both routes, after it had already completed its journey.

A delayed-choice experiment along these lines was carried out by Hellmuth, Walther, Zajonc and Schleich [1987] with an interferometer incorporating 5 m long single-mode fibers in the two paths. The light source was a mode-locked

krypton-ion laser emitting pulses with a duration of 150 ps at a repetition rate of 81 MHz. An acousto-optic switch was used to select one pulse out of 8000, thereby ensuring that the time between pulses was much longer than the transit time of the light through the interferometer. An optical attenuator reduced the average number of photons per pulse to less than 0.2. A combination of a Pockels cell and a polarizing prism was used as a switch in one arm to interrupt the light after it had passed the first beam splitter. Data were recorded as the mode of operation was switched between normal and delayed-choice for successive light pulses.

The results obtained showed no observable difference between the normal and delayed-choice modes of operation, in agreement with the predictions of quantum mechanics. However, since the picosecond pulse is in a coherent state, the second-order correlation function $g^{(2)}(0)$ is nonzero, and perfect path information cannot be obtained.

Another delayed-choice experiment, performed by Balduhn, Mohler and Martienssen [1989], used photon pairs produced by parametric down-conversion (see § 2.5.2). One photon served as a trigger to switch between registration of “which-path” information and phase information. In this case also, the result was independent of whether the switching took place before, or after, the photon passed the first beam splitter of the interferometer.

7.3. THE QUANTUM ERASER

Another consequence of the uncertainty principle is that any attempt to identify the path of a photon leads to an irreversible change in its momentum, which in turn washes out any interference effects (Bohr [1983]). However, measurements which do not involve a reduction of the state vector can be reversible in some sense.

Normally, whenever “which-path” information is available, the paths in an interferometer are no longer indistinguishable, and interference effects cannot be observed. However, interference effects may reappear if the distinguishing information can somehow be “erased” by correlating the results of the measurements with the results of properly chosen measurements on the physical system. This procedure is the basis of what is now commonly known as the “quantum eraser” (Scully and Druhl [1982], Scully, Englert and Walther [1991], Zajonc, Wang, Zou and Mandel [1991]).

One demonstration of a quantum eraser (Kwiat, Steinberg and Chiao [1992]) used the interferometer shown in fig. 7.1. A half-wave plate inserted in one of the paths before the beam splitter was used to rotate the plane of polarization

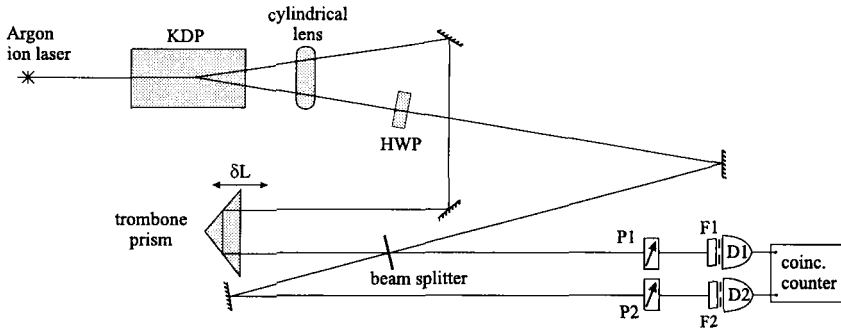


Fig. 7.1. Two-photon interferometer used as a quantum eraser (Kwiat, Steinberg and Chiao [1992]).

of one of the beams. When the polarization of this beam was orthogonal to that of the other beam, the coincidence null disappeared, since it became possible to identify the paths taken by each of the photons. However, this information could be erased by inserting two polarizers just in front of the photo detectors, after the photons had left the beam splitter.

In particular, if the initial polarization of the down-converted photons was horizontal, and the half-wave plate rotated one polarization to vertical, polarizers at 45° before each detector restored the original coincidence null. Interference could not be restored with a single polarizer in front of one detector, since “which-path” information was available from the photon reaching the other photodetector. In addition, as shown in fig. 7.2, if one polarizer was set at 45° and the other at -45° , an interference peak was observed instead of a dip.

The quantum-eraser concept could also be realized with the interferometer shown in fig. 6.7 (Ou, Wang, Zou and Mandel [1990]). In this case, removal of the beam splitter BS_B , which at first sight should not affect the results, destroyed the interference. The explanation is that since the signal and idler photons are produced simultaneously, it then became possible from the output of the photo detector D_B to decide whether the corresponding signal photon came from NL_1 or NL_2 . Insertion of BS_B mixed the idlers and erased the information on the paths taken by the photons (Zajonc, Wang, Zou and Mandel [1991]).

The experimental arrangement shown in fig. 6.10 (Zou, Wang and Mandel [1991]) could also be modified to demonstrate this concept by using a half-wave plate between the two crystals to rotate the polarization of the idler photons from NL_1 , so that it was orthogonal to the polarization of the idlers from NL_2 . In this arrangement, interference could be recovered by using a polarizer in front of D_i and correlating the counts of the two detectors.

With fast detectors and a rapidly switchable polarizer, it should even be

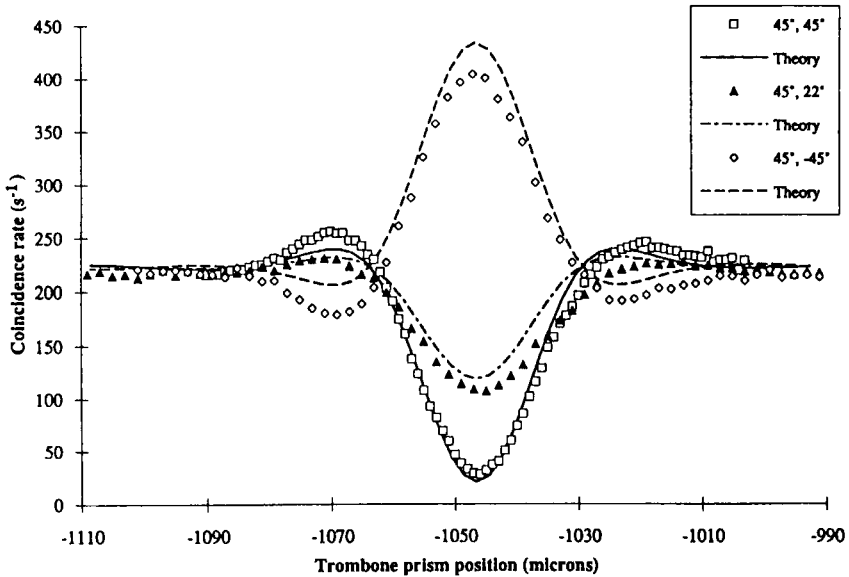


Fig. 7.2. Experimental data obtained with a two-photon interferometer with the polarizer in one path set at 45° and the polarizer in the other path set at various angles (Kwiat, Steinberg and Chiao [1992]).

possible to choose the orientation of the polarizer after the signal photon is detected, making possible a delayed-choice decision to observe particle-like behavior (“which-path” information) or wave-like behavior (interference) (Kwiat, Steinberg and Chiao [1994]).

In all these cases, it appears that the state vector reflects not only what is known about the photon, but also whatever information is available in principle. The additional measurements needed to obtain this information, either on the source or on the path of the detected photon, need not actually be carried out; it is enough for them to be possible, in principle, for the interference effects to be destroyed.

7.4. SINGLE-PHOTON TUNNELING

If two right-angle prisms are placed with their hypotenuse faces opposite each other, but separated by an air gap, a beam of light incident on the interface at an angle greater than the critical angle is totally internally reflected. However, if the air gap is reduced to a fraction of a wavelength, some of the light is transmitted.

The fact that light tunnels through such a gap by evanescent coupling confirms the wave-like behavior of light.

On the other hand, if the same experiment is repeated with single-photon states, nonclassical effects are observed (Ghose, Home and Agarwal [1991]). With this arrangement, as we have seen earlier, quantum mechanics predicts that photons will be detected in perfect anticoincidence in the transmitted and reflected beams. This prediction has been verified experimentally by Mizobuchi and Ohtake [1992]. Accordingly, we have a situation where single-photon states display wave-like properties (tunneling) as well as particle-like properties (anticoincidence).

7.4.1. Tunneling time

The phenomenon of tunneling is actually a fundamental consequence of quantum mechanics, which states that all quantum particles, in principle, can tunnel through normally forbidden regions of space. However, the question of how much time it takes for a particle to tunnel through a barrier is quite controversial (Büttiker and Landauer [1982], Hauge and Støvneng [1989], Fertig [1990]). Interferometric experiments have made it possible to study this aspect of photon tunneling.

7.4.2. Dispersion cancellation

It follows from the uncertainty principle that, to make measurements of transit times with high resolution, it is necessary to make the energy uncertainty or spectral bandwidth quite large. With such large spectral bandwidths, any dispersive effects can result in significant broadening of a pulse, and a consequent decrease in time resolution (Franson [1992]). This problem can be avoided by making measurements with correlated photon pairs. It is then possible to take advantage of quantum-mechanical effects to obtain an effective cancellation of dispersion (Steinberg, Kwiat and Chiao [1992a,b, 1993]).

With photon pairs produced in an entangled state, the frequencies of the individual photons are not defined sharply, but the sum of their frequencies is fixed. If we use an interferometer similar to that described by Hong, Ou and Mandel [1987] (see fig. 5.4), with a dispersive medium (say, a glass plate) in one beam, one photon of each pair travels through the dispersive medium while its conjugate travels through a path containing only air. However, after the photons are recombined at the beam splitter, it becomes impossible to determine which one of them travelled through the glass plate. This indistinguishability leads to

a cancellation of first-order dispersion effects, so that there is no broadening of the coincidence minimum. As a result, the shift in the position of the minimum in the rate of coincidences can be used to make high-resolution measurements of the propagation delay produced by the glass plate.

7.4.3. Measurements of tunneling time

The experimental arrangement used for measurements of tunneling time is shown in fig. 7.3 (Steinberg, Kwiat and Chiao [1993]). The tunnel barrier was a multilayer dielectric mirror consisting of 11 alternating layers of low- and high-index material, each a quarter of a wavelength thick at the wavelength used (700 nm in air), coated on one half of the surface of a high-quality optical flat. In such a periodic structure, the multiple reflections interfere so as to exponentially damp the incident wave, resulting in the equivalent of a photonic bandgap (Yablonovitch [1993]) at which more than 99% of the incident light is reflected.

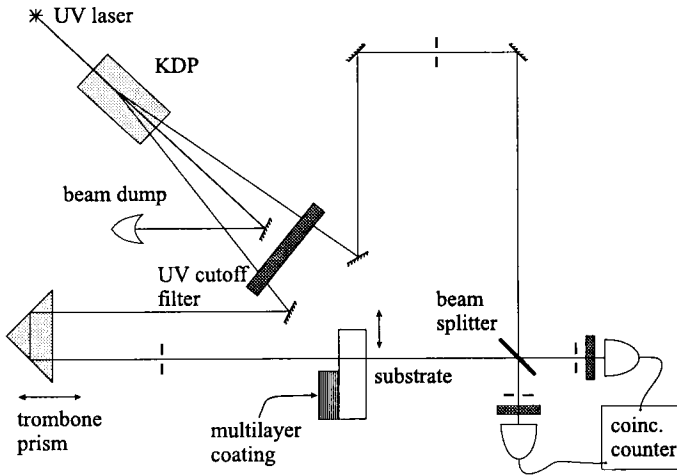


Fig. 7.3. Apparatus used for measurements of the single-photon tunneling time (Steinberg, Kwiat and Chiao [1993]).

To make measurements of the tunneling time, the multilayer structure was moved periodically into and out of the beam, while the optical path difference between the beams was varied slowly by translating the reflecting prism. A Gaussian curve was then fitted to each of the two dips in the rate of coincidences, and the distance between their centers was calculated. Figure 7.4

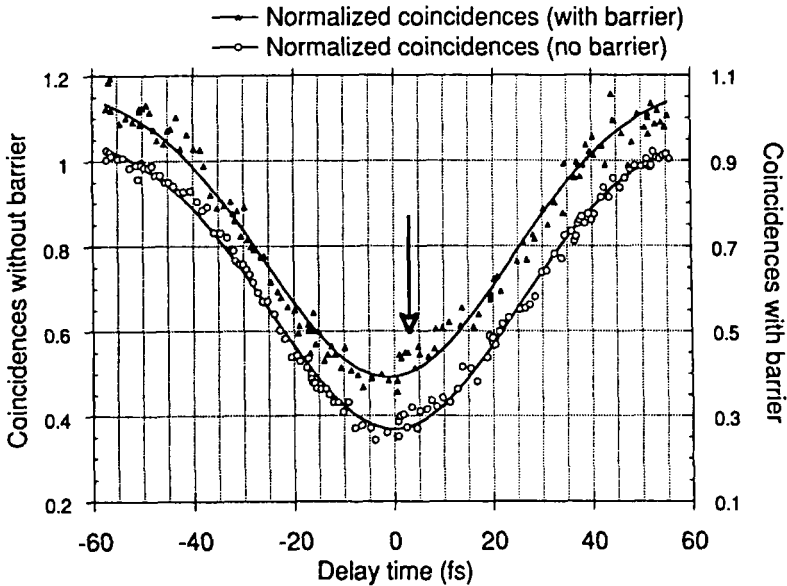


Fig. 7.4. Variation of the rate of coincidence counts with the delay time, with and without the tunnel barrier in the optical path. With the barrier, the minimum occurs approximately 2 fs earlier than without the barrier (Steinberg, Kwiat and Chiao [1993]).

shows a typical set of data. The average of several such measurements showed that the peak arrived 1.47 ± 0.21 fs earlier when the multilayer was in the path (Steinberg, Kwiat and Chiao [1993]). In an extension of this experiment, Steinberg and Chiao [1995] determined the delay times for the transmission of photons through a dielectric mirror as a function of the angle of incidence. These measurements made it possible to study the energy dependence of the tunneling time.

The interpretation of the apparently superluminal velocities observed has been discussed by Landauer [1993]. One explanation is that the whole transmitted wave packet comes from the leading edge of the much larger incident wave packet.

7.5. INTERACTION-FREE MEASUREMENTS

An interesting application of complementarity discussed by Elitzur and Vaidman [1993] and by Vaidman [1994] is in interaction-free measurements. At issue is the determination of whether or not a perfectly efficient detector occupies a certain region of space, without actually triggering this detector. To dramatize the

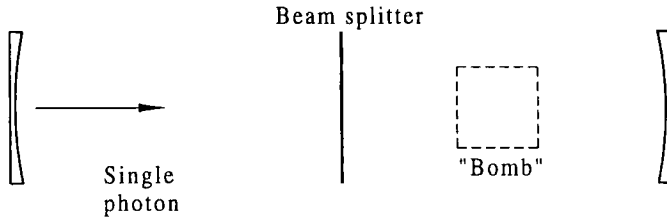


Fig. 7.5. Scheme for interaction-free measurements (Kwiat, Weinfurter, Herzog, Zeilinger and Kasevich [1995]).

situation, the detector is pictured as a bomb which has unit detection efficiency and is triggered by the absorption of a single photon; one must determine whether the bomb is present, or not, without allowing a single photon to be absorbed.

A Mach–Zehnder interferometer can be set up so that all photons exit through a specified output port if the detector, or bomb, is not located in one arm of the interferometer. The presence of the bomb in this arm destroys the interference required for all photons to exit only through the specified port. It follows that the presence of the bomb can be detected through the observation of a photon exiting from the other port. However, for an interferometer constructed with 50:50 beam splitters, the probability of triggering the bomb is 50%, while the probability of knowing unambiguously that the bomb is present, without triggering the bomb, is only 25%. Accordingly, while this scheme permits, in principle, interaction-free measurements of the presence of the bomb, it is far from ideal. The basic strategy for interaction-free measurements is, therefore, to exploit the wave-like behavior of light to increase the probability of establishing the presence of an absorber, while reducing, or eliminating, the probability of a photon traversing the path in which the absorber lies.

Kwiat, Weinfurter, Herzog, Zeilinger and Kasevich [1995] have proposed an interaction-free measurement scheme which, assuming a loss-free system, can raise this ratio for interaction-free measurements to as close to unity as desired. As shown in fig. 7.5, a beam splitter is placed in an optical cavity; the single photon is generated on one side of the beam splitter (say, the left) and the detector (the bomb) is placed on the other side. For a reflectivity

$$R = \cos^2\left(\frac{\pi}{2N}\right), \quad (7.2)$$

the photon will be found in the right side of the cavity, after N time cycles, with probability $\cos^2(\pi/2N)$ if the bomb is not present; however, if the bomb is present, the wave function of the photon is continually projected back on to the left half of the cavity, with the probability of finding the photon in the left half of the cavity, after N cycles, tending to unity as $N \rightarrow \infty$.

§ 8. Quantum Limits to Interferometry

8.1. NUMBER-PHASE UNCERTAINTY RELATION

Dirac [1927], in his formulation of quantum electrodynamics, quantized the field by treating the photon number n and phase ϕ as canonically conjugate quantities, rather than the variables X_1 and X_2 of eq. (2.17). However, quantization of the phase variable is not straightforward, due to the periodicity of the phase and the lower bound for the spectrum of the photon number operator (Susskind and Glogower [1964], Paul [1974]). Despite this difficulty, the number-phase uncertainty relation defined by eq. (7.1) has proved useful for characterizing the limited precision of phase measurements with laser light sources (Serber and Townes [1960], Friedburg [1960]). The inequality defined by eq. (7.1) quantifies the trade-off between reducing photon-number fluctuations in the source and reducing the phase noise, and the coherent state of light can be regarded as a minimum-uncertainty state in the strong-field limit (Carruthers and Nieto [1965, 1968]). The difficulty with the periodicity of the phase can be alleviated by replacing the phase operator by noncommuting operators corresponding to $\cos\phi$ and $\sin\phi$ (Louisell [1963], Susskind and Glogower [1964]), leading to a modified version of the uncertainty relation (7.1) involving Δn , $\Delta \cos\phi$ and $\Delta \sin\phi$.

Gerhardt, Welling and Frölich [1973] and Gerhardt, Buchler and Litfin [1974] attempted to measure directly the phase fluctuations of a microscopic radiation field, in order to check the number-phase uncertainty relation. They sent coherent light from a laser into a Mach-Zehnder interferometer and attenuated the light in one path to a mean photon number between 3 and 12. The resultant increase in phase fluctuations induced a random phase shift in the beam in that arm. This field was then amplified by a Q -switched laser with a gain factor of 10^{10} . The field in the second arm of the interferometer served as the reference field for homodyne detection of the output. In order to minimize external disturbances, the phase deviation between two pulses separated by less than a microsecond was measured. The results of these experiments did not agree with the uncertainty relations of Carruthers and Nieto [1965], but Nieto [1977] showed that they agreed better with measurements of a phase-difference operator, rather than with measurements of absolute phase.

It must be kept in mind that although direct measurements of phase, and, therefore, of number-phase uncertainty relations, cannot be performed, indirect measurements of phase are possible. Alternate versions of phase operators can be constructed for particular phase-sensitive measurements (Barnett and

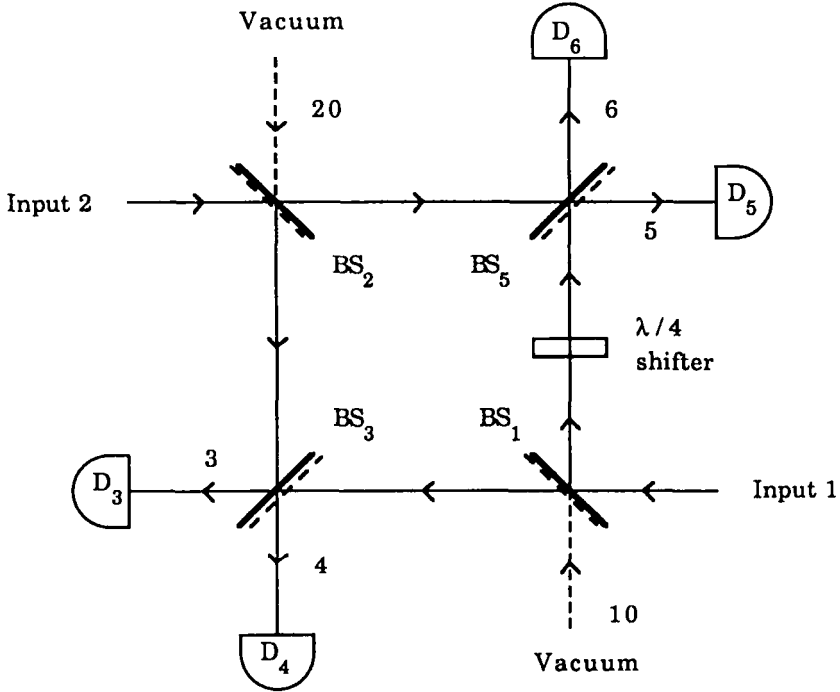


Fig. 8.1. Interferometer used to measure the phase difference between two beams of light (Noh, Fougères and Mandel [1991]).

Pegg [1986], Noh, Fougères and Mandel [1991, 1992a,b]) or inferred from measurements of quasiprobability distributions such as the Wigner function, as in the experiments performed by Smithey, Beck, Cooper and Raymer [1993].

The optical system used by Noh, Fougères and Mandel [1991, 1992a,b] is shown in fig. 8.1. In this arrangement, the two input fields are mixed by four beam splitters, and four photo detectors are used to count the photons emerging from four output ports. A 90° phase shifter is inserted in one arm of the interferometer.

For this measurement scheme, the cosine and sine operators can be taken to be

$$\begin{aligned}\widehat{C}_M &= (\hat{n}_4 - \hat{n}_3) [(\hat{n}_4 - \hat{n}_3)^2 + (\hat{n}_6 - \hat{n}_5)^2]^{-1/2}, \\ \widehat{S}_M &= (\hat{n}_6 - \hat{n}_5) [(\hat{n}_4 - \hat{n}_3)^2 + (\hat{n}_6 - \hat{n}_5)^2]^{-1/2},\end{aligned}\quad (8.1)$$

where n_3 , n_4 , n_5 and n_6 correspond to the photon counts registered by the detectors D_3 , D_4 , D_5 and D_6 , respectively. The operators describe the

measurement statistics well in the limit that the photon-number fluctuations at each detector are small compared to the mean photon number.

A theoretical analysis then shows that for input fields with $\langle \hat{n}_1 \rangle, \langle \hat{n}_2 \rangle \ll 1$, the dispersions of \hat{C}_M and \hat{S}_M obey the inequalities

$$\frac{\langle (\Delta \hat{C}_M)^2 \rangle^{1/2}}{|\langle \hat{C}_M \rangle|} \geq 1, \quad \frac{\langle (\Delta \hat{S}_M)^2 \rangle^{1/2}}{|\langle \hat{C}_M \rangle|} \geq 1, \quad (8.2)$$

so that both the cosine and the sine of the phase difference are ill-defined. This result is confirmed experimentally. The probability distribution $\mathcal{P}(\phi_2 - \phi_1)$ of the phase difference can then be derived by imposing a phase shift ϕ_s on the field at input port 2, and repeating the measurements for a range of values of ϕ_s from $-\pi$ to π .

8.2. THE STANDARD QUANTUM LIMIT

The quantum limit in interferometry is usually obtained from an argument which balances the error due to photon-counting statistics against the disturbances of the end mirrors produced by fluctuations in radiation pressure (Edelstein, Hough, Pugh and Martin [1978], Forward [1978]). According to this argument, since the number of photons which pass through the interferometer in the measurement time τ is

$$n = \frac{P\tau}{\hbar\omega}, \quad (8.3)$$

where P is the laser power, fluctuations in the laser power produce an uncertainty in n given by the relation

$$\Delta n \approx n^{-1/2}. \quad (8.4)$$

The existence of this quantum limit is now well established, but the argument leading to it has been open to question, since it relies on the assumption that the power fluctuations in the two arms are uncorrelated.

A more rigorous analysis (Caves [1980]) reveals two different, but equivalent, points of view on the origin of the fluctuations. The first attributes them to the fact that each photon incident on the beam splitter is scattered independently, thereby producing binomial distributions of photons in the two arms which are precisely anticorrelated. The second ascribes them to vacuum (zero-point)

fluctuations in the field entering the interferometer from the other input port. This field acts in antiphase on the laser fields in the two arms. It follows, therefore, that the photon-counting error is an intrinsic property of the interferometer.

The standard quantum limit (SQL) in interferometry is obtained by inserting eq. (8.4) into eq. (7.1) to obtain the corresponding uncertainty in the measured values of the phase:

$$\Delta\phi \geq \frac{1}{2\sqrt{\bar{n}}}, \quad (8.5)$$

where \bar{n} is the mean photon number. This limit poses problems in measuring extremely small displacements and is critical in such applications as the detection of gravitational waves. One way to overcome the SQL is by injecting squeezed states into one or both ports of the interferometer (Caves [1981], Bondurant and Shapiro [1984]).

8.3. INTERFEROMETRY BELOW THE SQL

A schematic of a Michelson interferometer designed to detect gravitational radiation (Caves [1980]) is shown in fig. 8.2. This interferometer uses a delay line in each arm, and although only two reflections on each mirror are shown, a larger number can be used to increase the effective length of each arm (Billing, Maischberger, Rüdiger, Schilling, Schnupp and Winkler [1979]). A change in the difference of the lengths of the optical paths in the two arms due to a gravitational wave results in a change in the phase difference between the beams, which can be measured by the intensity change at the detector.

The SQL can be overcome in such an interferometer by using squeezed light. A limit,

$$\Delta\phi \approx \frac{1}{\bar{n}}, \quad (8.6)$$

is achievable in principle by feeding suitably constructed squeezed states into both input ports of the interferometer. In actual experiments with a polarization interferometer, an increase in the signal-to-noise ratio of 2 dB, relative to the shot-noise limit, has been achieved using squeezed light generated by an optical parametric amplifier (Grangier, Slusher, Yurke and LaPorta [1987]). The maximum improvement in sensitivity can be obtained by preparing the light entering each of the two input ports of the interferometer in a state that consists of exactly j photons (Yurke, McCall and Klauder [1986], Holland and Burnett

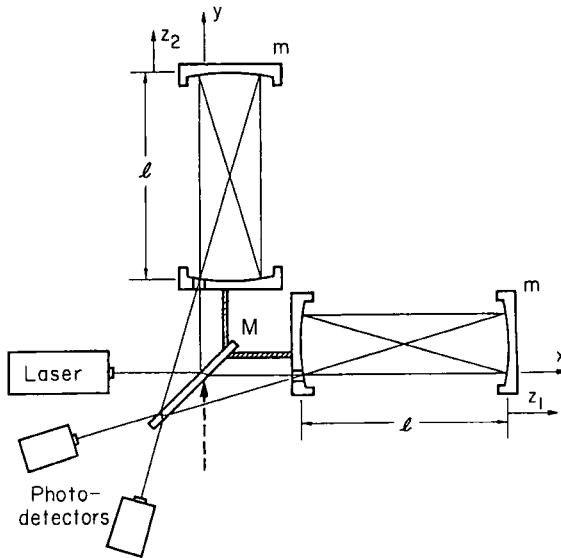


Fig. 8.2. Schematic of a Michelson interferometer for detecting gravitational waves (Caves [1980]).

[1993], Sanders and Milburn [1995]). States conforming to this requirement can be generated, for example, with two-mode four-wave mixers (Yurke, McCall and Klauder [1986]). The difference in the photo counts at the two output ports can then be processed to obtain the phase difference. However, to achieve maximum sensitivity, the deviation of the phase difference ϕ from zero must be less than $1/\bar{n}$. This requirement can be met by the use of a feedback loop that holds ϕ at zero.

8.4. INTERFEROMETERS USING ACTIVE ELEMENTS

An analysis based on the theory of Lie groups shows that conventional interferometers using only passive elements can be characterized by an $SU(2)$ -group symmetry. An alternative class of interferometers, characterized by an $SU(1, 1)$ -group symmetry (Yurke, McCall and Klauder [1986]), exploits the fact that the output of an active element, such as a four-wave mixer or degenerate parametric amplifier, depends on the relative phases of the pump and the incoming signal. In these interferometers, beam splitters are replaced by such active elements, and no light is fed into the input ports. They offer the possibility of attaining a phase sensitivity approaching $1/\bar{n}$ with fewer optical elements.

In one arrangement, the beam splitters of a conventional interferometer are replaced by four-wave mixers. When the two optical paths are equal, no light is delivered to the photodetectors, since the pairs of pump photons converted into pairs of four-wave output photons at the first four-wave mixer are converted back into pump photons at the second four-wave mixer. An alternative arrangement uses two degenerate parametric amplifiers. The output is then sensitive to the difference between the phases accumulated by the signal and pump beams.

§ 9. Conclusions

The dawn of the twentieth century saw the introduction of a duality to the behavior of light. Depending on the experiment chosen, light appeared to behave either as a wave or as a collection of particles. The quantum theory of light evolved in response to the need to reconcile these two contradictory aspects.

Starting from the early work of Dirac [1927] on the quantization of light, which treated photon number and phase as complementary quantities, and the use of coherent states of light to make the transition from classical to quantum descriptions of radiation, this progression led, eventually, to a single cohesive theory of quantum optics which has successfully described and predicted a diverse range of phenomena.

However, despite the success of quantum theory in explaining nonclassical effects, the mystery of the quantum world is deep enough to provoke many tests of the theory itself. Optical interferometry has played an increasingly important part in these tests, ranging from early experiments which verified Dirac's famous dictum to recent experiments involving Bell's inequality. In all these cases, optical interferometry has provided evidence supporting quantum theory and refuting alternative theories.

The mysterious aspects of quantum theory arise essentially because of the complementarity of wave and particle behavior. In the case of light, the complementarity of photon number and phase is still provoking research. The question of "What is phase?" has compelled researchers to conduct experiments to probe the limits to phase measurements, and theoreticians to ponder a definition of phase that is consistent with the axioms of quantum theory.

The duality inherent in the quantum description of light provides two alternate pictures for describing interference phenomena in an intuitive way: the "semi-classical picture", which treats the quantized light field as being composed of classical waves which can interact with quantized matter, and the "photon picture", which treats the light quanta as fundamental. Each picture has its

advantages and limitations, depending on the experiment considered, but the two pictures overlap in discussions of weak semiclassical fields where the number of photons is small, and individual photons can be detected.

In most situations, the “photon picture” gives a good description of the interference phenomena observed, provided that Dirac’s statement that “a photon interferes only with itself . . .” is borne in mind. There are conceptual difficulties in applying this dictum to some of the higher-order interference effects described in this review, but a way out is to extend it to read “each pair of photons interferes only with itself”.

An alternative explanation is to regard optical interference as due to the existence of indistinguishable paths; on this basis, the effects observed are explained as a manifestation of the correspondence between the mutual coherence and the indistinguishability of two light beams (Mandel [1991]). We can then apply Feynman’s rules for interference, after taking into account the fact that outcomes which are distinguishable, even in principle, do not interfere. In all other cases, the coherent addition of the probability amplitudes associated with each path, and the evaluation of the squared modulus of this sum, yields the probability of detection of a photon. This far-reaching principle appears to provide an intuitive understanding of all interference effects.

References

- Adam, A., L. Janossy and P. Varga, 1955a, *Acta Phys. Hung.* **4**, 301.
 Adam, A., L. Janossy and P. Varga, 1955b, *Ann. Phys. (N.Y.)* **16**, 408.
 Agarwal, G.S., and P. Hariharan, 1993, *Opt. Commun.* **103**, 111.
 Alford, W.P., and A. Gold, 1958, *Am. J. Phys.* **26**, 481.
 Arecchi, F.T., A. Berné and P. Burlamacchi, 1966, *Phys. Rev. Lett.* **16**, 32.
 Aspect, A., J. Dalibard and G. Roger, 1982, *Phys. Rev. Lett.* **49**, 1804.
 Aspect, A., and P. Grangier, 1987, *Hyperfine Interactions* **37**, 3.
 Aspect, A., P. Grangier and G. Roger, 1981, *Phys. Rev. Lett.* **47**, 460.
 Baldzuhn, J., E. Mohler and W. Martienssen, 1989, *Z. Phys. B* **77**, 347.
 Barnett, S.M., and D.T. Pegg, 1986, *J. Phys. A* **19**, 3849.
 Bell, J.S., 1965, *Physics* **1**, 195.
 Berry, M.V., 1984, *Proc. R. Soc. (London) A* **392**, 45.
 Berry, M.V., 1987, *J. Mod. Opt.* **34**, 1401.
 Bhandari, R., and J. Samuel, 1988, *Phys. Rev. Lett.* **60**, 1211.
 Billing, H., K. Maischberger, A. Rüdiger, R. Schilling, L. Schnupp and W. Winkler, 1979, *J. Phys.* **E 12**, 1043.
 Bohm, D., 1951, *Quantum Theory* (Prentice Hall, Englewood Cliffs, NJ) p. 614.
 Bohr, N., 1983, in: *Quantum Theory and Measurement*, eds J.A. Wheeler and W.H. Zurek (Princeton University Press, Princeton, NJ) p. 32.
 Bondurant, R.S., and J.H. Shapiro, 1984, *Phys. Rev. D* **30**, 2458.

- Braginsky, V.B., 1989, in: 3rd Int. Symp. on Foundation of Quantum Mechanics in the Light of New Technology, eds S. Kobayashi, H. Ezawa, Y. Murayama and S. Nomura (The Physical Society of Japan, Tokyo) p. 135.
- Brendel, J., W. Dultz and W. Martienssen, 1995, *Phys. Rev. A* **52**, 2551.
- Brendel, J., E. Mohler and W. Martienssen, 1991, *Phys. Rev. Lett.* **66**, 1142.
- Brendel, J., E. Mohler and W. Martienssen, 1992, *Europhys. Lett.* **20**, 575.
- Brendel, J., S. Schüttrumpf, R. Lange, W. Martienssen and M.O. Scully, 1988, *Europhys. Lett.* **5**, 223.
- Burnham, D.C., and D.L. Weinberg, 1970, *Phys. Rev. Lett.* **25**, 84.
- Büttiker, M., and R. Landauer, 1982, *Phys. Rev. Lett.* **49**, 1739.
- Campos, R.A., B.E.A. Saleh and M.C. Teich, 1989, *Phys. Rev. A* **40**, 1371.
- Carruthers, P., and M.M. Nieto, 1965, *Phys. Rev. Lett.* **14**, 387.
- Carruthers, P., and M.M. Nieto, 1968, *Rev. Mod. Phys.* **40**, 411.
- Casabella, P.A., and T. Gonsiorowski, 1980, *Am. J. Phys.* **48**, 393.
- Caves, C.M., 1980, *Phys. Rev. Lett.* **45**, 75.
- Caves, C.M., 1981, *Phys. Rev. D* **23**, 1693.
- Caves, C.M., and B.L. Schumaker, 1985, *Phys. Rev. D* **31**, 3068.
- Chiao, R.Y., 1970, *Phys. Lett. A* **33**, 177.
- Chiao, R.Y., A. Antaramian, K.M. Ganga, H. Jiao, S.R. Wilkinson and H. Nathel, 1988, *Phys. Rev. Lett.* **60**, 1214.
- Chyba, T.H., L.J. Wang, L. Mandel and R. Simon, 1988, *Opt. Lett.* **13**, 562.
- Clauser, J.F., 1974, *Phys. Rev. D* **9**, 853.
- Clauser, J.F., M.A. Horne, A. Shimony and R.A. Holt, 1969, *Phys. Rev. Lett.* **23**, 880.
- Clauser, J.F., and A. Shimony, 1978, *Rep. Prog. Phys.* **41**, 1881.
- Croca, J.R., A. Garuccio, V.L. Lepore and R.N. Moreira, 1990, *Found. Phys. Lett.* **3**, 557.
- de Broglie, L., 1969, *The Current Interpretation of Wave Mechanics* (Elsevier, Amsterdam).
- Dempster, A.J., and H.F. Batho, 1927, *Phys. Rev.* **30**, 644.
- Diedrich, F., and H. Walther, 1987, *Phys. Rev. Lett.* **58**, 203.
- Dirac, P.A.M., 1927, *Proc. R. Soc. (London) A* **114**, 243.
- Dirac, P.A.M., 1958, *The Principles of Quantum Mechanics*, 4th Ed. (Oxford University Press, Oxford) p. 9.
- Eberhard, P.H., 1993, *Phys. Rev. A* **47**, R747.
- Edelstein, W.A., J. Hough, J.R. Pugh and W. Martin, 1978, *J. Phys. E* **11**, 710.
- Einstein, A., B. Podolsky and N. Rosen, 1935, *Phys. Rev.* **47**, 777.
- Elitzur, A.C., and L. Vaidman, 1993, *Found. Phys.* **23**, 987.
- Fearn, H., and R. Loudon, 1987, *Opt. Commun.* **64**, 485.
- Fearn, H., and R. Loudon, 1989, *J. Opt. Soc. Am. B* **6**, 917.
- Ferguson, J.B., and R.H. Morris, 1978, *Appl. Opt.* **17**, 2924.
- Fertig, H.A., 1990, *Phys. Rev. Lett.* **65**, 2321.
- Feynman, R.P., R.B. Leighton and M. Sands, 1963, *Lectures on Physics*, Vol. 3 (Addison-Wesley, London) ch. 3.
- Forrester, A.T., R.A. Gudmundsen and P.O. Johnson, 1955, *Phys. Rev.* **99**, 1691.
- Forward, R.L., 1978, *Phys. Rev. D* **17**, 379.
- Franson, J.D., 1989, *Phys. Rev. Lett.* **62**, 2205.
- Franson, J.D., 1991a, *Phys. Rev. Lett.* **67**, 290.
- Franson, J.D., 1991b, *Phys. Rev. A* **44**, 4552.
- Franson, J.D., 1992, *Phys. Rev. A* **45**, 3126.
- Freedman, S.J., and J.F. Clauser, 1972, *Phys. Rev. Lett.* **28**, 938.
- Friberg, S., C.K. Hong and L. Mandel, 1985, *Phys. Rev. Lett.* **54**, 2011.

- Friedburg, H., 1960, in: *Quantum Electronics*, ed. C.H. Townes, (Columbia University Press, New York) p. 228.
- Gans, R., and P. Miguez, 1917, *Ann. Phys.* **52**, 291.
- Gerhardt, H., U. Buchler and G. Litfin, 1974, *Phys. Lett. A* **49**, 119.
- Gerhardt, H., H. Welling and D. Frölich, 1973, *Appl. Phys.* **2**, 91.
- Ghose, P., D. Home and G.S. Agarwal, 1991, *Phys. Lett. A* **153**, 403.
- Ghosh, R., C.K. Hong, Z.Y. Ou and L. Mandel, 1986, *Phys. Rev. A* **34**, 3962.
- Ghosh, R., and L. Mandel, 1987, *Phys. Rev. Lett.* **59**, 1903.
- Glauber, R.J., 1963a, *Phys. Rev.* **130**, 2529.
- Glauber, R.J., 1963b, *Phys. Rev.* **131**, 2766.
- Grangier, P., A. Aspect and J. Vigué, 1985, *Phys. Rev. Lett.* **54**, 418.
- Grangier, P., G. Roger and A. Aspect, 1986, *Europhys. Lett.* **1**, 173.
- Grangier, P., R.E. Slusher, B. Yurke and A. LaPorta, 1987, *Phys. Rev. Lett.* **59**, 2153.
- Grayson, T.P., J.R. Torgerson and G.A. Barbosa, 1994, *Phys. Rev. A* **49**, 626.
- Hanbury Brown, R., 1974, *The Intensity Interferometer* (Taylor and Francis, London).
- Hanbury Brown, R., and R.Q. Twiss, 1956, *Nature (London)* **177**, 27.
- Hardy, L., 1992a, *Phys. Rev. Lett.* **68**, 2981.
- Hardy, L., 1992b, *Phys. Lett. A* **167**, 17.
- Hardy, L., 1993, *Phys. Rev. Lett.* **71**, 1665.
- Hariharan, P., N. Brown, I. Fujima and B.C. Sanders, 1993, *J. Mod. Opt.* **40**, 1477.
- Hariharan, P., N. Brown, I. Fujima and B.C. Sanders, 1995, *J. Mod. Opt.* **42**, 565.
- Hariharan, P., N. Brown and B.C. Sanders, 1993, *J. Mod. Opt.* **40**, 113.
- Hariharan, P., and M. Roy, 1992, *J. Mod. Opt.* **39**, 1811.
- Hariharan, P., M. Roy, P.A. Robinson and J.W. O'Byrne, 1993, *J. Mod. Opt.* **40**, 871.
- Haroche, S., M. Brune and J.M. Raimond, 1992, in: *13th Int. Conf. on Atomic Physics*, AIP Conf. Proc. **275**, 261.
- Harris, S.E., M.K. Oshman and R.L. Byer, 1967, *Phys. Rev. Lett.* **18**, 732.
- Hauge, E.H., and J.A. Støvneng, 1989, *Rev. Mod. Phys.* **61**, 917.
- Heitler, W., 1954, *The Quantum Theory of Radiation*, 3rd Ed. (Oxford University Press, London).
- Hellmuth, T., H. Walther, A. Zajonc and W. Schleich, 1987, *Phys. Rev. A* **35**, 2532.
- Herzog, T., J.G. Rarity, H. Weinfurter and A. Zeilinger, 1994, *Phys. Rev. Lett.* **72**, 629.
- Holland, M.J., and K. Burnett, 1993, *Phys. Rev. Lett.* **71**, 1355.
- Holland, P.R., and J.P. Vigié, 1991, *Phys. Rev. Lett.* **67**, 402.
- Hong, C.K., and L. Mandel, 1985, *Phys. Rev. A* **31**, 2409.
- Hong, C.K., and L. Mandel, 1986, *Phys. Rev. Lett.* **56**, 58.
- Hong, C.K., Z.Y. Ou and L. Mandel, 1987, *Phys. Rev. Lett.* **59**, 2044.
- Horne, M.A., A. Shimony and A. Zeilinger, 1989, *Phys. Rev. Lett.* **62**, 2209.
- Imoto, N., H.A. Haus and Y. Yamamoto, 1985, *Phys. Rev. A* **32**, 2287.
- Janossy, L., and Z. Naray, 1957, *Acta Phys. Acad. Sci. Hung.* **7**, 403.
- Javan, A., E.A. Ballik and W.L. Bond, 1962, *J. Opt. Soc. Am.* **52**, 96.
- Jerrard, H.G., 1954, *J. Opt. Soc. Am.* **44**, 634.
- Jordan, T.F., 1994, *Phys. Rev. A* **50**, 62.
- Jordan, T.F., and F. Ghielmetti, 1964, *Phys. Rev. Lett.* **12**, 607.
- Kimble, H.J., and D.F. Walls, 1987, *J. Opt. Soc. Am. B* **4**, 1450.
- Kitagawa, M., and Y. Yamamoto, 1986, *Phys. Rev. A* **34**, 3974.
- Klyshko, D.N., 1967, *JETP Lett.* **6**, 23.
- Kocher, C.A., and E.D. Commins, 1967, *Phys. Rev. Lett.* **18**, 575.
- Kwiat, P.G., and R.Y. Chiao, 1991, *Phys. Rev. Lett.* **66**, 588.
- Kwiat, P.G., P. Eberhard, A.M. Steinberg and R.Y. Chiao, 1994, *Phys. Rev. A* **49**, 3209.

- Kwiat, P.G., A.M. Steinberg and R.Y. Chiao, 1992, *Phys. Rev. A* **45**, 7729.
- Kwiat, P.G., A.M. Steinberg and R.Y. Chiao, 1993, *Phys. Rev. A* **47**, R2472.
- Kwiat, P.G., A.M. Steinberg and R.Y. Chiao, 1994, *Phys. Rev. A* **49**, 61.
- Kwiat, P.G., A.M. Steinberg, R.Y. Chiao, P. Eberhard and M. Petroff, 1993, *Phys. Rev. A* **48**, R867.
- Kwiat, P.G., W.A. Vareka, C.K. Hong, H. Nathel and R.Y. Chiao, 1990, *Phys. Rev. A* **41**, 2910.
- Kwiat, P.G., H. Weinfurter, T. Herzog, A. Zeilinger and M.A. Kasevich, 1995, *Phys. Rev. Lett.* **74**, 4763.
- Landauer, R., 1993, *Nature* **365**, 692.
- Larchuk, T.S., R.A. Campos, J.G. Rarity, P.R. Tapster, E. Jakeman, B.E.A. Saleh and M.C. Teich, 1993, *Phys. Rev. Lett.* **70**, 1603.
- Lee, B., E. Yin, T.K. Gustafson and R.Y. Chiao, 1992, *Phys. Rev. A* **45**, 4319.
- Louisell, W.H., 1963, *Phys. Lett.* **7**, 60.
- Maeda, M.W., P. Kumar and J.H. Shapiro, 1987, *Opt. Lett.* **12**, 161.
- Magyar, G., and L. Mandel, 1963, *Nature* **198**, 255.
- Mandel, L., 1962, *J. Opt. Soc. Am.* **52**, 1335.
- Mandel, L., 1964, *Phys. Rev.* **134**, A10.
- Mandel, L., 1976, in: *Progress in Optics*, Vol. 13, ed. E. Wolf (North-Holland, Amsterdam) p. 27.
- Mandel, L., 1982, *Phys. Lett. A* **89**, 325.
- Mandel, L., 1983, *Phys. Rev. A* **28**, 929.
- Mandel, L., 1991, *Opt. Lett.* **16**, 1882.
- Mandel, L., and E. Wolf, 1965, *Rev. Mod. Phys.* **37**, 231.
- Milburn, G.J., 1984, *J. Phys. A* **17**, 737.
- Milburn, G.J., and D.F. Walls, 1983, *Phys. Rev. A* **28**, 2065.
- Mizobuchi, Y., and Y. Ohtake, 1992, *Phys. Lett. A* **168**, 1.
- Morris, R.H., J.B. Ferguson and J.S. Warniak, 1975, *Appl. Opt.* **14**, 2808.
- Newton, T.D., and E.P. Wigner, 1949, *Rev. Mod. Phys.* **21**, 400.
- Nieto, M.M., 1977, *Phys. Lett. A* **60**, 401.
- Noh, J.W., A. Fougères and L. Mandel, 1991, *Phys. Rev. Lett.* **67**, 1426.
- Noh, J.W., A. Fougères and L. Mandel, 1992a, *Phys. Rev. A* **45**, 424.
- Noh, J.W., A. Fougères and L. Mandel, 1992b, *Phys. Rev. A* **46**, 2840.
- Ou, Z.Y., 1988, *Phys. Rev. A* **37**, 1607.
- Ou, Z.Y., C.K. Hong and L. Mandel, 1987, *Opt. Commun.* **63**, 118.
- Ou, Z.Y., and L. Mandel, 1988a, *Phys. Rev. Lett.* **61**, 50.
- Ou, Z.Y., and L. Mandel, 1988b, *Phys. Rev. Lett.* **61**, 54.
- Ou, Z.Y., L.J. Wang, X.Y. Zou and L. Mandel, 1990, *Phys. Rev. A* **41**, 566.
- Ou, Z.Y., X.Y. Zou, L.J. Wang and L. Mandel, 1990a, *Phys. Rev. Lett.* **65**, 321.
- Ou, Z.Y., X.Y. Zou, L.J. Wang and L. Mandel, 1990b, *Phys. Rev. A* **42**, 2957.
- Pancharatnam, S., 1956, *Proc. Indian Acad. Sci. A* **44**, 247. Reprinted: 1975, in: *Collected Works of S. Pancharatnam*, (Oxford University Press, Oxford) p. 77.
- Paul, H., 1974, *Fortschr. Phys.* **22**, 657.
- Paul, H., 1986, *Rev. Mod. Phys.* **58**, 209.
- Pavičić, M., 1994, *Phys. Rev. A* **50**, 3486.
- Pavičić, M., 1995, *J. Opt. Soc. Am. B* **12**, 821.
- Pavičić, M., and J. Summhammer, 1994, *Phys. Rev. Lett.* **73**, 3191.
- Pflegeor, R.L., and L. Mandel, 1967a, *Phys. Lett. A* **24**, 766.
- Pflegeor, R.L., and L. Mandel, 1967b, *Phys. Rev.* **159**, 1084.
- Pflegeor, R.L., and L. Mandel, 1968, *J. Opt. Soc. Am.* **58**, 946.
- Pipkin, F.M., 1978, in: *Advances in Atomic and Molecular Physics*, Vol. 14, eds D.R. Bates and B. Bederson (Academic Press, New York) p. 281.

- Ramaseshan, S., and R. Nityananda, 1986, *Curr. Sci. (India)* **55**, 1225.
- Rarity, J.G., and P.R. Tapster, 1989, *J. Opt. Soc. Am. B* **6**, 1221.
- Rarity, J.G., and P.R. Tapster, 1990, *Phys. Rev. Lett.* **64**, 2495.
- Rarity, J.G., and P.R. Tapster, 1992, *Phys. Rev. A*, **45**, 2054.
- Rarity, J.G., P.R. Tapster, E. Jakeman, T. Larchuk, R.A. Campos, M.C. Teich and B.E.A. Saleh, 1990, *Phys. Rev. Lett.* **65**, 1348.
- Roch, J.F., G. Roger, P. Grangier, J. Courty and S. Reynaud, 1992, *Appl. Phys. B* **55**, 291.
- Sanders, B.C., and G.J. Milburn, 1989, *Phys. Rev. A* **39**, 694.
- Sanders, B.C., and G.J. Milburn, 1995, *Phys. Rev. Lett.* **75**, 2944.
- Santos, E., 1992, *Phys. Rev. A* **46**, 3646.
- Scully, M.O., and K. Druhl, 1982, *Phys. Rev. A* **25**, 2208.
- Scully, M.O., B.-G. Englert and H. Walther, 1991, *Nature* **351**, 111.
- Serber, R., and C.H. Townes, 1960, in: *Quantum Electronics*, ed. C.H. Townes (Columbia University Press, New York) p. 233.
- Shelby, R.M., M.D. Levenson, S.H. Perlmuter, R.G. de Voe and D.F. Walls, 1986, *Phys. Rev. Lett.* **57**, 691.
- Shih, Y.H., and C.O. Alley, 1988, *Phys. Rev. Lett.* **61**, 2921.
- Shih, Y.H., A.V. Sergienko and M.H. Rubin, 1993, *Phys. Rev. A* **47**, 1288.
- Simon, R., H.J. Kimble and E.C.G. Sudarshan, 1988, *Phys. Rev. Lett.* **61**, 19.
- Slusher, R.E., L.W. Hollberg, B. Yurke, J.C. Mertz and J.F. Valley, 1985, *Phys. Rev. Lett.* **55**, 2409.
- Smithy, D.T., M. Beck, J. Cooper and M.G. Raymer, 1993, *Phys. Rev. A* **48**, 3159.
- Steinberg, A.M., and R.Y. Chiao, 1995, *Phys. Rev. A* **51**, 3525.
- Steinberg, A.M., P.G. Kwiat and R.Y. Chiao, 1992a, *Phys. Rev. Lett.* **68**, 2421.
- Steinberg, A.M., P.G. Kwiat and R.Y. Chiao, 1992b, *Phys. Rev. A* **45**, 6659.
- Steinberg, A.M., P.G. Kwiat and R.Y. Chiao, 1993, *Phys. Rev. Lett.* **71**, 708.
- Sudarshan, E.C.G., 1963, *Phys. Rev. Lett.* **10**, 277.
- Susskind, L., and J. Glogower, 1964, *Physics* **1**, 49.
- Taylor, G.I., 1909, *Proc. Cambridge Philos. Soc.* **15**, 114.
- Tiwari, S.C., 1992, *J. Mod. Opt.* **39**, 1097.
- Tomita, A., and R.Y. Chiao, 1986, *Phys. Rev. Lett.* **57**, 937.
- Torgerson, J.R., D. Branning and L. Mandel, 1995, *Appl. Phys. B* **60**, 267.
- Torgerson, J.R., D. Branning, C.H. Monken and L. Mandel, 1995, *Phys. Lett. A* **204**, 323.
- Vaidman, L., 1994, *Quantum Opt.* **6**, 119.
- Vain'shtein, L.A., V.N. Melekhin, S.A. Mishin and E.R. Podolyak, 1981, *Sov. Phys. JETP* **54**, 1054.
- Vigué, J., J.A. Beswick and M. Broyer, 1983, *J. Phys. (Paris)* **44**, 1225.
- Vigué, J., P. Grangier, G. Roger and A. Aspect, 1981, *J. Phys. (Paris)* **42**, L531.
- von Weiszäcker, C.F., 1931, *Z. Phys.* **70**, 114.
- Walls, D.F., 1977, *Am. J. Phys.* **45**, 952.
- Walls, D.F., 1983, *Nature* **306**, 141.
- Walther, H., 1992, in: *13th Int. Conf. on Atomic Physics*, AIP Conf. Proc. **275**, 287.
- Wang, L.J., X.Y. Zou and L. Mandel, 1991, *Phys. Rev. Lett.* **66**, 1111.
- Wheeler, J.A., 1978, in: *Mathematical Foundations of Quantum Theory*, ed. A.R. Marlow (Academic Press, New York) p. 9.
- Wolf, E., 1955, *Proc. R. Soc. (London)* **230**, 246.
- Wootters, W.K., and W.H. Zurek, 1979, *Phys. Rev. D* **19**, 473.
- Wu, L., H.J. Kimble, J.L. Hall and H. Wu, 1986, *Phys. Rev. Lett.* **57**, 2520.
- Yablonovitch, E., 1993, *J. Opt. Soc. Am. B* **10**, 283.
- Yamamoto, Y., N. Imoto and S. Machida, 1986, in: *2nd Int. Symp. on Foundations of Quantum*

- Mechanics in the Light of New Technology, eds S. Kobayashi, H. Ezawa, Y. Murayama and S. Nomura (The Physical Society of Japan, Tokyo) p. 265.
- Yuen, H.P., 1976, *Phys. Rev. A* **13**, 2226.
- Yurke, B., S.L. McCall and J.R. Klauder, 1986, *Phys. Rev. A* **33**, 4033.
- Zajonc, A.G., L.J. Wang, X.Y. Zou and L. Mandel, 1991, *Nature* **353**, 507.
- Zeeman, P., 1925, *Physica (The Hague)* **5**, 325.
- Zou, X.Y., T.P. Grayson, G.A. Barbosa and L. Mandel, 1993, *Phys. Rev. A* **47**, 2293.
- Zou, X.Y., T.P. Grayson and L. Mandel, 1992, *Phys. Rev. Lett.* **69**, 3041.
- Zou, X.Y., L.J. Wang and L. Mandel, 1991, *Phys. Rev. Lett.* **67**, 318.